nature microbiology

ARTICLES

https://doi.org/10.1038/s41564-019-0631-2

Control of nitrogen fixation in bacteria that associate with cereals

Min-Hyung Ryu[1], Jing Zhang[1], Tyler Toth[1], Devanshi Khokhani[2], Barney A. Geddes[3], Florence Mus[4,5], Amaya Garcia-Costas[4,6], John W. Peters[4,5], Philip S. Poole[3], Jean-Michel Ané[2] and Christopher A. Voigt[1*]

Legumes obtain nitrogen from air through rhizobia residing in root nodules. Some species of rhizobia can colonize cereals but do not fix nitrogen on them. Disabling native regulation can turn on nitrogenase expression, even in the presence of nitrogenous fertilizer and low oxygen, but continuous nitrogenase production confers an energy burden. Here, we engineer inducible nitrogenase activity in two cereal endophytes (*Azorhizobium caulinodans* ORS571 and *Rhizobium* sp. IRBG74) and the well-characterized plant epiphyte *Pseudomonas protegens* Pf-5, a maize seed inoculant. For each organism, different strategies were taken to eliminate ammonium repression and place nitrogenase expression under the control of agriculturally relevant signals, including root exudates, biocontrol agents and phytohormones. We demonstrate that *R.* sp. IRBG74 can be engineered to result in nitrogenase activity under free-living conditions by transferring a *nif* cluster from either *Rhodobacter sphaeroides* or *Klebsiella oxytoca*. For *P. protegens* Pf-5, the transfer of an inducible cluster from *Pseudomonas stutzeri* and *Azotobacter vinelandii* yields ammonium tolerance and higher oxygen tolerance of nitrogenase activity than that from *K. oxytoca*. Collectively, the data from the transfer of 12 *nif* gene clusters between 15 diverse species (including *Escherichia coli* and 12 rhizobia) help identify the barriers that must be overcome to engineer a bacterium to deliver a high nitrogen flux to a cereal crop.

Nitrogen is a limiting nutrient that needs to be added as fertilizer in agriculture, including cereals, that cannot obtain it from the atmosphere. In contrast, legumes obtain most of their nitrogen through mutualism with nitrogen-fixing rhizobia that reside in root nodules. The majority of global calories are from cereals; hence, it has been a long-standing dream to transfer this ability to these crops[1,2]. This would reduce the need for nitrogenous fertilizer and the economic, environmental and energy burdens that it brings[3]. One solution is to engineer the bacteria that associate with cereals—whether they are in the soil, on the root surface (epiphytes) or living inside the roots (endophytes)—to fix nitrogen[4].

Some of the rhizobia isolated from legume root nodules are also cereal endophytes[5–8]; however, most are unable to fix nitrogen under free-living conditions (outside of the nodule)[9,10]. There have been reports of improvements in cereal yield due to these bacteria, including a 20% increase for rice by *Rhizobium* sp. IRBG74, but this is probably due to other mechanisms such as improved nutrient uptake or phytohormone production[9,11–35]. *Azorhizobium caulinodans* ORS571 is exceptional because it is able to fix nitrogen in both aerobic free-living and symbiotic states, has been shown to be a rice and wheat endophyte, and does not need plant metabolites to make functional nitrogenase[28,36–40]. However, when *Rhizobium* or *Azorhizobium* species are living in cereal roots, there is low nitrogenase expression and the $^{15}N_2$-transfer rates suggest the uptake is probably due to bacterial death[9,11–30]. To date, it has not been shown that a *Rhizobium* strain can be engineered to fix nitrogen under free-living conditions when it does not do so naturally.

Several bacterial species are used as cereal seed inoculants that either fix nitrogen naturally or are potential hosts into which the capability could be transferred. The non-host-specific endophyte *Pseudomonas stutzeri* and epiphyte *Klebsiella oxytoca* can colonize rice and wheat and be used to improve growth[41–47]. The epiphyte *Pseudomonas protegens* Pf-5 is used as a commercial biocontrol seed inoculant for maize and rice but it cannot fix nitrogen[48,49].

Nitrogen fixation (*nif*) genes are organized in clusters, ranging from an 11 kb operon in *Paenibacillus* to 64 kb spread across multiple loci in *A. caulinodans*. Conserved genes include those encoding nitrogenase (*nifHDK*) and cofactor (FeMoCo) biosynthesis[50–55]. Species that fix nitrogen under more conditions tend to have larger clusters with environment-specific paralogues, alternative electron transport routes and oxygen-protective mechanisms[50–61]. There is strong evidence for the lateral transfer of *nif* clusters between species[62,63]. However, engineering such a transfer poses a challenge, as many things can go awry, including regulation, missing genes and different intracellular conditions[10,56,64–66]. Since the first transfer in 1972 from *K. oxytoca* to *Escherichia coli*, additional clusters have been transferred to *E. coli* as well as between pseudomonads and *Paenibacillus* to *Bacilli*[61,66–75].

Nif genes are under stringent regulatory control due to its draw on metabolic and energy resources: nitrogenase can make up 20% of the cell mass and each ammonium requires approximately 40 ATP for its production[76,77]. Thus, it is strongly repressed by fixed nitrogen. Nitrogenase is also oxygen sensitive and its transcription is repressed under aerobic conditions. These signals converge on the NifA regulator, which partners with the sigma factor RpoN[55,76–79]. Additional species-specific and often poorly understood signals—which include plant-produced chemicals, ATP, reducing power, temperature and carbon sources—control these regulators[66,76–78,80–84].

[1]Synthetic Biology Center, Department of Biological Engineering, Massachusetts Institute of Technology, Cambridge, MA, USA. [2]Departments of Bacteriology and Agronomy, University of Wisconsin–Madison, Madison, WI, USA. [3]Department of Plant Sciences, University of Oxford, Oxford, UK. [4]Department of Chemistry and Biochemistry, Montana State University, Bozeman, MT, USA. [5]Institute of Biological Chemistry, Washington State University, Pullman, WA, USA. [6]Department of Biology, Colorado State University–Pueblo, Pueblo, CO, USA. *e-mail: cavoigt@gmail.com

Bacteria that can fix nitrogen under more conditions tend to have more complex regulation[10,76–78].

When a *nif* cluster is transferred between species and is functional, it either preserves its regulation by environmental stimuli or shows an unregulated constitutive phenotype[56,66,70,75]. Maintaining the native regulation, notably ammonium repression, limits their use in agriculture because such levels are likely to fluctuate according to soil types, irrigation and fertilization[85–87]. Nitrogen-fixing bacteria have been engineered to reduce ammonium sensitivity by disrupting NifL[88–90], mutating NifA[91–94] or transcribing the cluster using T7 RNA polymerase (RNAP)[70–73,93–95]. The constitutive expression of nitrogenase is also undesirable, as it imparts a fitness burden on the cells[16,96]. A notable example is the transfer of a *nif* cluster to *P. protegens* Pf-5, which led to ammonium secretion but resulted in a rapid decline in the bacterial population in the soil[75,97]. Constitutive activity is detrimental even before the bacteria are introduced to the soil, impacting production, formulation and long-term storage[12,49,82,98–100].

Here, we present strategies to control nitrogen fixation in bacteria that live on or inside cereal roots. We evaluate native and engineered clusters from diverse sources that were transferred to many species, thus enabling side-by-side comparisons of activity. Regulatory control was achieved by replacing the regulatory control of clusters with synthetic regulation engineered to reduce ammonium repression. Of these, the most promising candidates are *A. caulinodans* (native cluster) and *P. protegens* Pf-5 (with the *Azotobacter vinelandii* cluster), which achieve high levels of inducible nitrogenase activity with reduced oxygen sensitivity. The regulatory control is replaced by synthetic, genetically encoded sensors that can keep *nif* transcription off at undesirable times and turn it on when needed. This includes sensors that respond to natural root exudates, chemicals released by soil bacteria and agricultural biocontrol agents[9,39,40,101–114]. Finally, plants can be engineered to release chemical signals from their roots, such as opines and rhizopine[115–117], and we demonstrate the ability to control *nif* with the former. Collectively, this work presents an unprecedented comparison of diverse natural and engineered nitrogen-fixing bacteria.

Results

Performance of native *nif* clusters in *E. coli*, *P. protegens* Pf-5 and symbiotic rhizobia. Native *nif* clusters from diverse species were cloned to compare their relative performance in different strain backgrounds (Fig. 1a). The list spans diverse bacterial orders—including Enterobacterales, Pseudomonadales, Rhizobiales, Rhodobacterales, Rhodospirillales, Bacillales and Oscillatoriales—and published cluster boundaries were used when available[62,70,118–124]. Some choices had to be made regarding which regions within the *nif* cluster to exclude or which genomic regions external to the cluster to include. A region (Pst1307–Pst1312) that does not impact activity[62] was excluded from the *P. stutzeri* A1501 cluster. In some cases, genes required for electron transport located outside of the cluster were fused to it (*rnf1*/*fix* for *A. vinelandii* DJ and *rnf* for *Rhodobacter sphaeroides* 2.4.1)[59,122,125–128]. This approach was also taken to fuse the required PatB regulator with the *Cyanothece* sp. ATCC51142 *nif* cluster[129]. The clusters were built by DNA synthesis or fragments amplified from genomic DNA, fused using yeast assembly and cloned into host-appropriate plasmid backbones (Methods). Fig. 1a shows the clusters that were functional in at least one host (those found to be non-functional, *Gluconacetobacter diazotrophicus*[130–132] and *A. caulinodans*[37], are shown in Supplementary Fig. 1).

The set of ten *nif* clusters were transferred into *E. coli* MG1655, the cereal epiphyte *P. protegens* Pf-5 and the cereal endophyte *R.* sp. IRBG74 to create 30 strains (Fig. 1b). *E. coli* and *P. protegens* Pf-5 neither fix nitrogen nor contain *nif* genes, but transfer experiments have been shown to be successful in these hosts[66,67,70]. Interestingly, *R.* sp. IRBG74 contains two *nif* clusters but does not fix nitrogen under free-living conditions. Noting that it lacks the required *nifV*[133], we tested whether this could be complemented just by adding *nifV* from *A. caulinodans* ORS571, but these experiments were unsuccessful (Extended Data Fig. 1). We therefore attempted to obtain activity by transferring the complete heterologous clusters into this host, leaving the native clusters intact.

The strains containing transferred *nif* clusters were cultured and evaluated for nitrogenase activity using an acetylene reduction assay (Methods). Each species required different growth conditions, media and carbon sources. *E. coli* was cultured under anaerobic conditions but the metabolisms of *P. protegens* Pf-5 and *R.* sp. IRBG74 require oxygen[34,134]; the initial headspace was thus set to 1% oxygen. The cells were incubated for 20 h at 30 °C in the presence of excess acetylene. There was little cell growth during this period; the activities for the different strains are therefore reported in arbitrary units at a defined cell density. These values closely correspond to specific nitrogenase activities (nmol ethylene min^{-1} mg^{-1} protein; see Methods).

A surprising seven of ten clusters were functional in *E. coli*, with the *K. oxytoca* cluster being the most active (Fig. 1b). This cluster was also functional in *P. protegens* Pf-5, albeit with a 60-fold lower activity. Interestingly, the clusters from *P. stutzeri* and *A. vinelandii*—both obligate aerobes—were highly active in *P. protegens* Pf-5. Only a single gene cluster from *R. sphaeroides* was active in *R.* sp. IRBG74 (Fig. 1b). Notably, both *Rhizobium* and *Rhodobacter* are alphaproteobacteria and their *nif* clusters may contain interchangeable genes. When the native *nif* clusters were knocked out of *R.* sp. IRBG74, introduction of the *R. sphaeroides* cluster did not lead to activity (Extended Data Fig. 1). These data point to a complex complementation between the endogenous and introduced gene clusters. To determine whether this approach could be generalized to other symbiotic rhizobia, the *R. sphaeroides* and *R. palustris* gene clusters were transferred to a panel of 12 species isolated from diverse legumes (Fig. 1b). This led to detectable activity in seven strains. However, we decided not to pursue this route further because of low activity and the difficulty in implementing control over the multiple clusters.

Next, we characterized the contribution of transcription and translation to the observed species barriers. When a cluster is transferred, the underlying genetic parts (promoters, ribosome binding sites (RBSs) and terminators) and codon usage of the genes could perturb the expression of the *nif* genes, which can be detrimental to activity. RNA sequencing (RNA-seq) was used to quantify the transcriptional parts when the *K. oxytoca nif* cluster was transferred to *E. coli*, *P. protegens* Pf-5 and *R. sp*. IRBG74. The transcription of the cluster was very similar when compared between *K. oxytoca* and *E. coli* (Fig. 2a,b), the ratio between the messenger RNAs was preserved (coefficient of multiple correlation (R^2 = 0.89; Fig. 2c) and the activity was indeed similar. In contrast, the transcriptional profiles differed considerably when this cluster was transferred to *P. protegens* Pf-5 and *R.* sp. IRBG74 (Fig. 2a,b), and there was no correlation between the mRNA transcripts (Fig. 2c).

Ribosome profiling measures the ribosome density on transcripts, from which one can quantify the protein-synthesis rate, RBS strength, ribosome pausing and relative expression levels in multiprotein complexes[135–137]. The translation efficiency is calculated by normalizing the ribosome density by the number of transcripts obtained from RNA-seq. Ribosome profiling was performed for the transfer of the *K. oxytoca nif* cluster to different hosts (Fig. 2d,e and Extended Data Fig. 2). The ratios between the protein expression rates in *K. oxytoca* were consistent with immunoblotting assays[138] and the known stoichiometry of NifHDK[139] (Supplementary Fig. 2). Unlike the mRNA levels, the ratios of the expression rates correlated strongly when the cluster was transferred between species: *E. coli* (R^2 = 0.94), *P. protegens* Pf-5 (R^2 = 0.61) and *R.* sp. IRBG74 (R^2 = 0.71; Fig. 2e). Noting that the rates of protein expression were

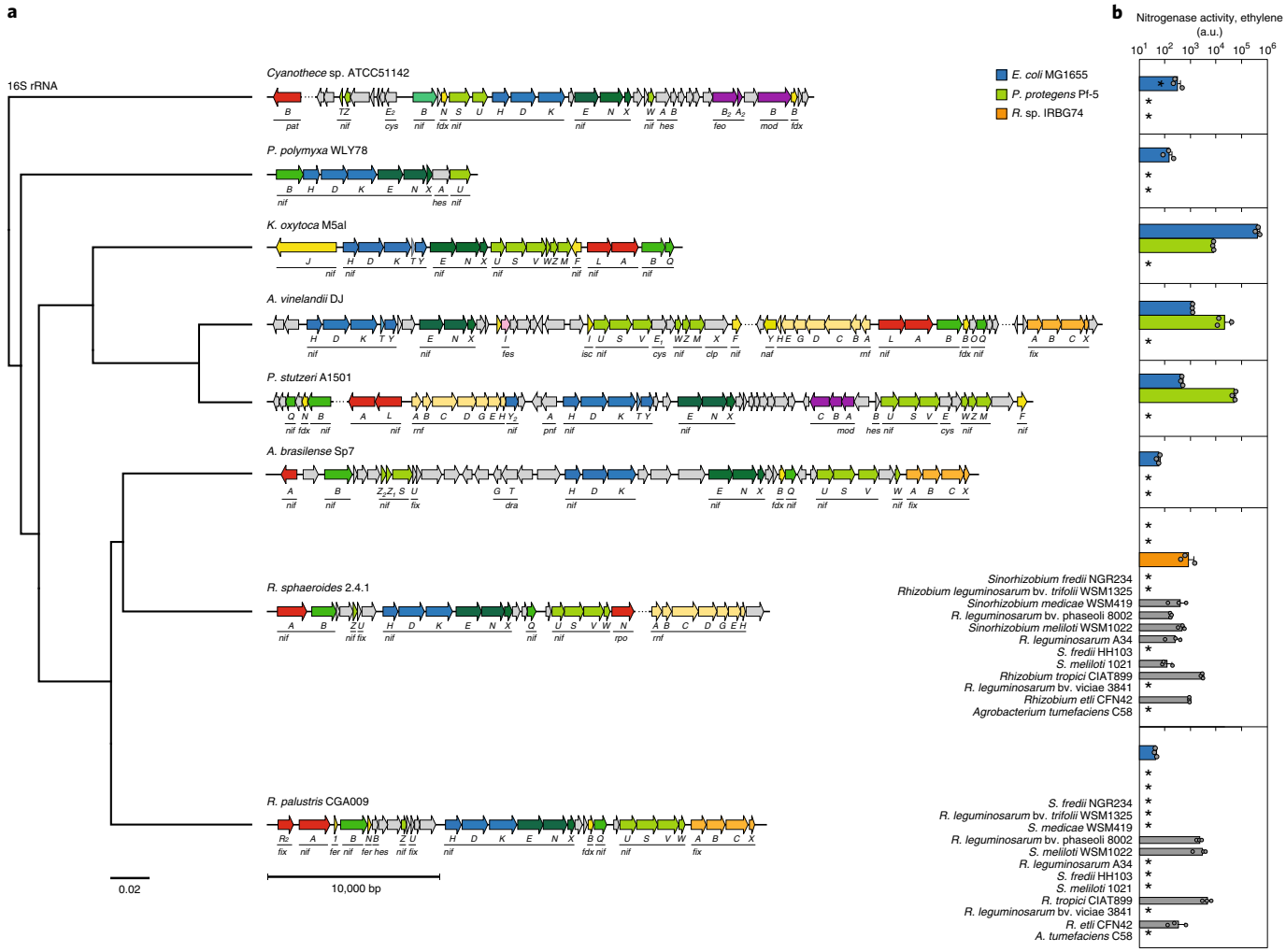

Fig. 1 | Transfer of *nif* clusters across species. a, Alignment of eight *nif* clusters from free-living nitrogen-fixing bacteria based on the phylogenetic relationships of the 16S rRNA sequences. The genes are coloured by function and operons based on *K. oxytoca* M5al: blue, structural components; green, cofactor biosynthesis (the shading corresponds to operons); yellow, electron transport (light and dark yellow indicate the *rnf* and *fix* operons, respectively); red, regulatory genes; purple, transporters and grey, unknown related to nitrogen fixation. The dots on the DNA line indicate where multiple regions were cloned from genomic DNA and combined to form one large plasmid-borne *nif* cluster. The boundaries of all of the *nif* clusters are provided in Supplementary Table 1, and the plasmids containing the *nif* clusters are provided in Supplementary Table 3. **b**, The nitrogenase activity from the transfer of the native *nif* clusters was measured in three species. The activities of the *Rhodopseudomonas palustris* and *R. sphaeroides nif* clusters were also measured in 12 rhizobia (grey). A complete list of the strain genotypes is provided in Supplementary Table 2. The asterisks indicate ethylene production at levels below the detection limit. The error bars represent the s.d. from three independent experiments performed on different days. a.u., arbitrary units.

lower in *R.* sp. IRBG74, we attempted to increase the expression of the *nif* gene to gain activity but this proved unsuccessful (Extended Data Fig. 3).

Considering the transfer experiments, the most successful recipient was *E. coli*. However, this is not a viable agricultural strain and activity was eliminated in the presence of ammonium (Extended Data Fig. 4)[66,67,140]. Moderately high activity could be obtained in *P. protegens* Pf-5 but this was either constitutively on (the *K. oxytoca* cluster) or ammonium-sensitive (the *A. vinelandii* cluster; Fig. 5e). In our hands, the *P. stutzeri* cluster in *P. protegens* Pf-5 was strongly repressed by ammonium, in disagreement with published results[75]. The transfer of clusters to rhizobia consistently led to low activity. We therefore sought to engineer the clusters to be more active, less sensitive to ammonium and inducible by exogenous signals.

Transfer of refactored *K. oxytoca nif* clusters to *R.* sp. IRBG74. The aim of genetic refactoring is to eliminate native regulation so that a system can be placed under the control of synthetic sensors and circuits[95,141–143]. To do this, genes are recoded to eliminate internal regulation, native parts (for example, RBSs) are replaced with those that have been well characterized and T7 RNAP promoters are used. A separate 'controller' connects sensors to the expression of T7 RNAP. This simplifies the change of stimuli that turn on a cluster to select a new controller, as long as it sweeps through the same dynamic range of T7 RNAP expression. We previously refactored the *K. oxytoca nif* cluster (v2.1), which produced the same activity despite significant genetic reorganization[71,72]. To transfer the cluster into *E. coli*, we designed a controller based on the isopropyl-β-D-thiogalactoside (IPTG)-inducible T7 RNAP carried on a plasmid (pKT249; Fig. 3a).

Because we had difficulty transferring activity with a native *nif* cluster into *R.* sp. IRBG74, we tried to move the v2.1 cluster. This required a new controller to be built for rhizobia. Although some inducible systems and sets of genetic parts have been previously described for rhizobia[144–151], we found that they did not achieve the required dynamic ranges. To this end, we characterized

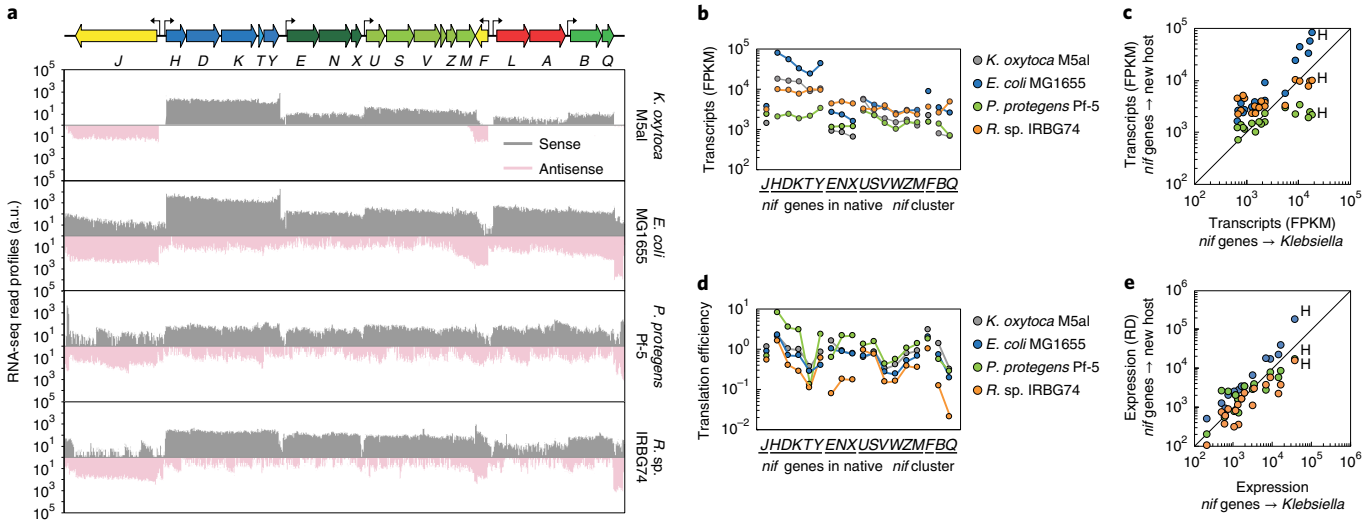

Fig. 2 | Transfer of the native *K. oxytoca nif* cluster across species. a, Transcriptomic profile of the native *K. oxytoca nif* cluster in *K. oxytoca* compared with those obtained from its transfer to the indicated species. **b**, Transcription levels of the native *K. oxytoca nif* cluster across species. The lines connect points that occur in the same operon. **c**, Transcription levels of the *K. oxytoca nif* genes ($n=18$) in *K. oxytoca* (→*Klebsiella*) compared with those obtained when transferred to a new host: *E. coli* ($R^2=0.89$, two-sided $P<0.0001$), *P. protegens* Pf-5 ($R^2<0$) and *R.* sp. IRBG74 ($R^2<0$). **d**, Same as in **b**, except the translational efficiencies, calculated using ribosome profiling, are compared. **e**, Same as in **c**, except the ribosome densities, calculated using ribosome profiling, are compared: *E. coli* ($R^2=0.94$, two-sided $P<0.00001$), *P. protegens* Pf-5 ($R^2=0.61$, two-sided $P=0.00013$) and *R.* sp. IRBG74 ($R^2=0.71$, two-sided $P=0.00001$). The R^2 values in the log–log plots were calculated from the line $y=x+b$, where b is an expression variable between hosts. H, *nifH*.

20 constitutive promoters[152] and seven T7 RNAP-dependent promoters[71] (Supplementary Fig. 3). We next screened a library of 285 computationally designed RBSs, which span a 5,600-fold expression range (Supplementary Fig. 4a; see Methods)[153]. Finally, 29 terminators[154,155] were characterized (Supplementary Fig. 5a). These part libraries were used to construct six inducible systems for *R.* sp. IRBG74 that respond to IPTG, 3OC6HSL, anhydrotetracycline (aTc), cuminic acid, 2,4-diacetylphloroglucinol (DAPG) and salicylic acid (Supplementary Fig. 6). After optimization, these systems generated a 7- to 400-fold induction of promoter activities in response to inducer treatments.

A controller was encoded in the genome based on the use of the IPTG sensor to express a low-toxicity variant of T7 RNAP[156] (Fig. 3a and Supplementary Fig. 8). The resulting response function spans a similar dynamic range to that obtained for pKT249 in *E. coli* (Fig. 3b). To achieve the same level of induction between the two species, 0.1 mM IPTG was selected for *E. coli* and 0.5 mM for *R.* sp. IRBG74 (circled points in Fig. 3b). This should set the same level of transcription between species; however, no activity was observed when we transferred v2.1 into *R.* sp. IRBG74 containing the controller (Fig. 3c,d). We performed RNA-seq and ribosome-profiling experiments to determine whether any genetic parts were misfunctioning (Supplementary Fig. 9). This demonstrated that the promoters were systematically less active (particularly those transcribing *nifH*), terminators misfunctioned and the translation rates differed between genes (Fig. 3e,f). There was almost no correlation when the expression rates of the *nif* genes were compared with their native levels in *K. oxytoca* (Fig. 3g).

Based on these results, we designed a new refactored cluster v3.2 (Fig. 3h). A very strong promoter was chosen for *nifH*. Promoters were added to divide *nifENX* and *nifJ*, and stronger terminators were selected. Operons and translational coupling have been proposed to be important in preserving expression ratios during evolutionary lateral transfer[157–159]. Thus, we hypothesized that the expression ratios are better preserved when the native cluster is transferred into a new host due to these features (Fig. 2d). To preserve this structure, we cloned the *K. oxytoca* operons intact and replaced these regions of the refactored cluster (Fig. 3h). Note that this also preserves *nifT* and *nifX*, which were not included in the first versions.

The v3.2 cluster is less active than v2.1 in *E. coli*. However, it is active in *R.* sp. IRBG74 and *P. protegens* Pf-5, in which v2.1 is completely inactive (Fig. 3i and Supplementary Fig. 10). Further, this activity occurs in the double knockout of *R.* sp. IRBG74 that lacks the *nif* clusters (Δ*nif*Δ*hsdR*). Ribosome profiling and RNA-seq were used to evaluate the performance of v3.2 in all three species (Fig. 3j–l, Supplementary Fig. 11 and Extended Data Fig. 5). The translation rates of the genes were remarkably similar to those observed for *K. oxytoca*, particularly for NifH (Fig. 3l). The higher expression of *nifH* and the preserved ratios between proteins are the probable reasons why the refactored cluster is functional in *R.* sp. IRBG74. However, the activity was low and increasing the inducer concentration demonstrated that there is an optimum beyond which there is a rapid decline in activity (Fig. 3m).

Replacement of *A. caulinodans nif* regulation with synthetic control. The *A. caulinodans nif* cluster is difficult to engineer because it is large (64 kb total, 76 genes), distributed across multiple loci and has a complex regulatory network[37,160–164]. Despite repeated efforts, we failed to move the clusters to *R.* sp. IRBG74 (Supplementary Fig. 1 and Extended Data Figs. 1b, 3) and refactoring was complicated by their size and the lack of gene-function information. We therefore decided to modify the regulation controlling *nif* so that it can be placed under the control of synthetic sensors.

Our initial goal was to eliminate the ammonium repression of nitrogenase activity, which converges on NifA[80,164]. To place *nifA* under inducible control (Fig. 4a), we first knocked out the genomic copy, which greatly reduced *nif* expression (Fig. 4b). The IPTG-inducible system designed for rhizobia was tested in *A. caulinodans* and found to work well (Supplementary Fig. 12). The expression of NifA leads to the induction of the *nifH* promoter and this is enhanced by the co-expression of RpoN (genomic *rpoN* was left intact). The response function from the *nifH* promoter was analysed at the condition used for nitrogen fixation, exhibiting a wide dynamic range of 45-fold (Fig. 4c). When the controller co-expressing NifA and RpoN

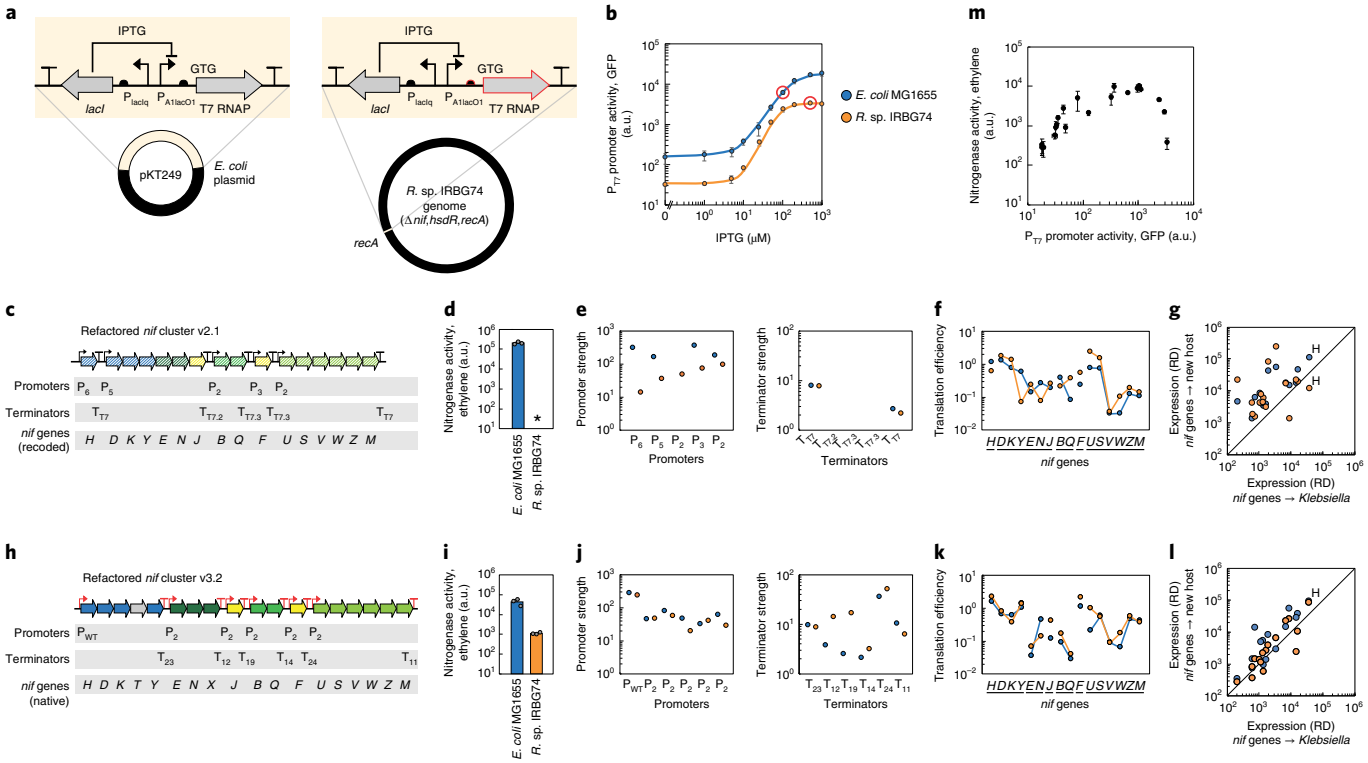

Fig. 3 | Transfer of the refactored *K. oxytoca nif* clusters to *R.* sp. IRBG74. a, Genetic systems for the controller for *E. coli* MG1655 (left) and *R.* sp. IRBG74 (right). A variant of T7 RNAP (R6232S, N-terminal Lon tag, GTG start codon) was used for the *E. coli* controller. Several genetic parts were substituted to build the *R.* sp. IRBG74 controller (red). The sequences for the genetic parts are provided in Supplementary Table 4. **b**, Response functions for the controllers with the reporter plasmid pMR80 (Supplementary Table 3). The IPTG concentrations used to induce nitrogenase are circled in red. **c**, Genetic parts used to build the refactored *nif* gene cluster v2.1 (Supplementary Table 4). **d**, Activity of the refactored *nif* gene cluster v2.1 in different hosts. The asterisk indicates ethylene production at levels below the detection limit. **e**, Activities of the refactored v2.1 promoters (left) and terminators (right) in *E. coli* MG1655 (blue) and *R.* sp. IRBG74 (orange), as calculated from RNA-seq data (see Methods). **f**, Translation efficiency of the v2.1 *nif* genes in *E. coli* MG1655 (blue) and *R.* sp. IRBG74 (orange), as calculated using ribosome profiling and RNA-seq. The lines connect points that occur in the same operon. **g**, Comparison of the ribosome density (RD) of the refactored v2.1 *nif* genes ($n=16$) in a new host versus that measured for the *nif* genes from the native *K. oxytoca* cluster in *K. oxytoca* (→*Klebsiella*). *E. coli*, $R^2=0.51$ and two-sided $P=0.002$; and *R.* sp. IRBG74, $R^2<0$; H, *nifH*. **h**,**i**,**j**,**k**,**l**, Same as **c**,**d**,**e**,**f**,**g**, respectively, but with the refactored *nif* cluster v3.2. **h**, The changes to the genetic components are shown in red. The genetic components are provided in Supplementary Table 4. **l**, *E. coli*, $R^2=0.63$ and two-sided $P=0.0002$; *R.* sp. IRBG74, $R^2=0.78$ and two-sided $P=0.00004$. **m**, Nitrogenase activity as a function of the T7-promoter strength. The refactored *nif* cluster v3.2 was expressed from three controller strains of *R.* sp. IRBG74 with varying strengths (Supplementary Fig. 8). The error bars represent the s.d. from three independent experiments on different days. The R^2 values in log–log plots were calculated from the line $y=x+b$, where b is an expression variable between hosts.

was induced, there was a complete recovery of activity (Fig. 4d). Growth by nitrogen fixation was also observed in ammonium-free agarose slopes under inducing conditions (see Methods; Fig. 4e).

The wild-type strain was strongly repressed by ammonium and even when NifA or RpoN are under inducible control the activity was reduced by 95% (Fig. 4f and Extended Data Fig. 6a). This suggests that the post-transcriptional control of NifA activity by ammonium remains intact[164,165]. NifA mutations that abrogate ammonium repression have been identified in related alphaproteobacteria, and we identified the equivalent positions to mutate in *A. caulinodans* (L94Q and D95Q) using a multiple sequence alignment (Supplementary Fig. 13)[93,94]. Co-expression of the NifA double mutant with RpoN recovered 50% of the activity in the presence of ammonium (Fig. 4f and Extended Data Fig. 6a).

The inducible *nif* cluster was then tested for oxygen sensitivity, noting that *A. caulinodans* is an obligate aerobe and fixes nitrogen under micro-aerobic conditions[37]. The tolerance of nitrogenase to oxygen was assessed as a function of the concentration of oxygen in the headspace, which was held constant by injecting oxygen while monitoring its level (see Methods and Supplementary Fig. 14). The native and inducible gene clusters responded nearly identically to oxygen, with an optimum of 0.5–1% and a broad tolerance (Fig. 4g and Extended Data Fig. 6b).

Controllable *nif* activity in *P. protegens* Pf-5. The native *K. oxytoca*, *P. stutzeri* and *A. vinelandii nif* clusters are all functional in *P. protegens* Pf-5 (Fig. 1a,b). However, either *nif* is strongly repressed by ammonium (*P. stutzeri* and *A. vinelandii*) or it is constitutively on (*K. oxytoca*; Fig. 5d,e). For these clusters, we sought to gain regulatory control by removing the *nifA* master regulators and expressing them from a controller (Fig. 5a).

Part libraries had to be built for *P. protegens* Pf-5 before we could construct controllers with a sufficient dynamic range. Our work compliments recent work to characterize the genetic-part libraries and inducible systems of pseudomonads[166–168]. We characterized 20 constitutive promoters, seven T7 promoters and 10 terminators (Supplementary Figs. 3 and 5b). A library of 192 RBSs was screened, encompassing a 4,079-fold range of expression (Supplementary Fig. 4b). The inducible systems designed for *Rhizobium* were transferred as is to a *Pseudomonas*-specific pRO1600-ori plasmid (see Methods). The DAPG, aTc, 3OC6HSL and cuminic acid sensors were all found to be functional and new sensors were built and optimized

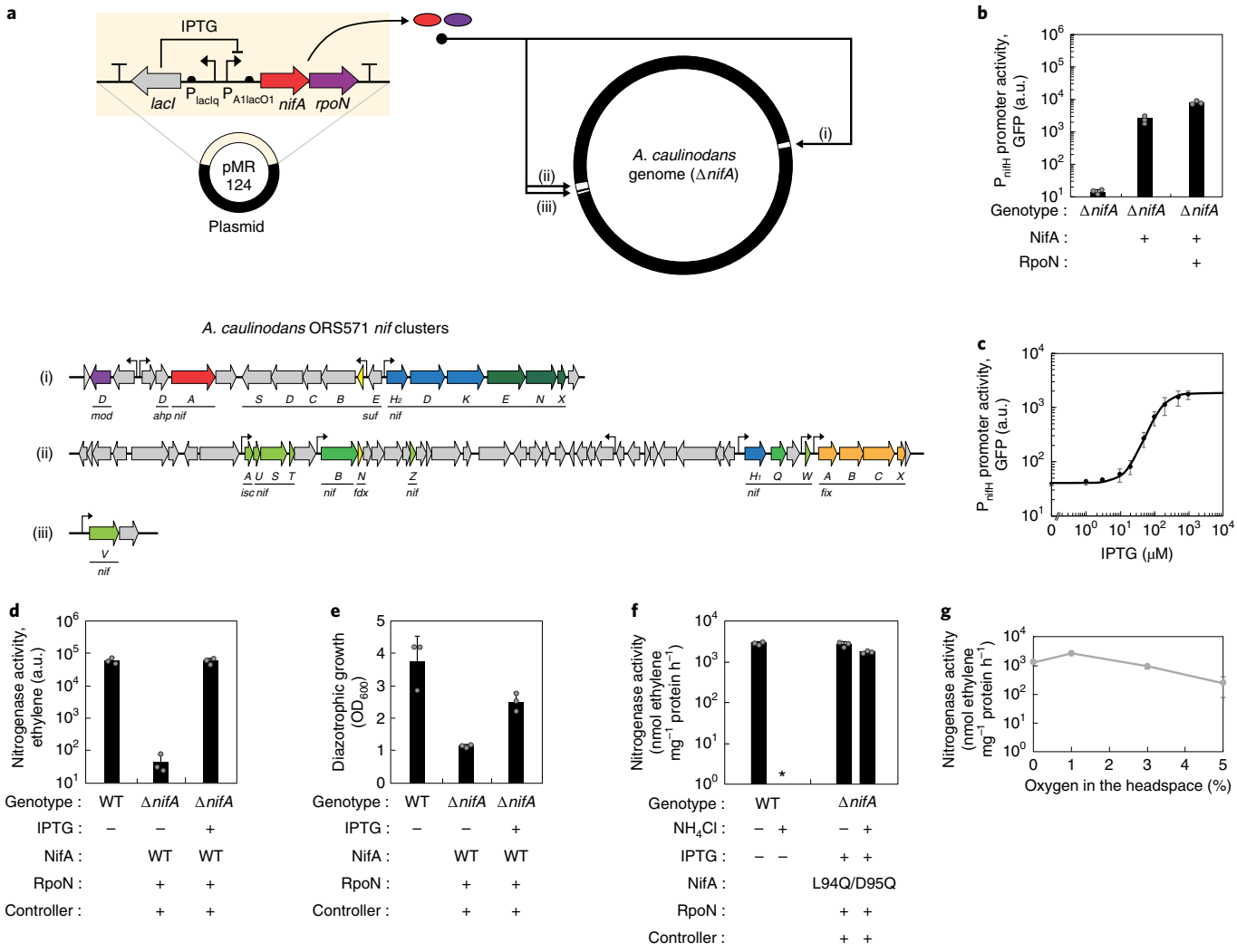

Fig. 4 | Control of nitrogen fixation in *A. caulinodans* ORS571. a, Schematic of the controller carried on the plasmid pMR124 (top left; genetic parts are provided in Supplementary Table 4). NifA and RpoN co-induce the expression of three sites in the genome ((i)–(iii), top right and bottom; identified by consensus NifA binding sequences). **b**, The levels of expression induced by the *nifH* promoter were evaluated using a fluorescent reporter (see Methods). NifA and RpoN were complemented individually or in combination in the *A. caulinodans* Δ*nifA*, where the genomic *rpoN* remains intact. **c**, Response function for the induction of the *nifH* promoter by the controller under nitrogen-fixing conditions (see Methods). **d**, Nitrogenase activity of wild-type *A. caulinodans* ORS571 compared with Δ*nifA* complemented with the controller plasmid and the addition of 1 mM IPTG. **e**, Same as in **d**, but the cell growth in ammonium-free agarose slopes is shown. **f**, Effect of the absence or presence of 10 mM ammonium chloride on the specific nitrogenase activity (see Methods). NifA and RpoN expression was induced with 1 mM IPTG for *A. caulinodans* Δ*nifA* containing the controller plasmid pMR127. The asterisk indicates ethylene production at levels below the detection limit. **g**, Specific nitrogenase activity of the inducible version encoding the controller shown as a function of the oxygen concentration in the headspace in the presence of 1 mM IPTG (see Methods). The error bars represent the s.d. from three independent experiments performed on different days. WT, wild type.

to respond to naringenin, arabinose and IPTG (Supplementary Fig. 7). These ranged from 41- to 554-fold induction.

We sought to build a single, universal controller that could induce the clusters from all three species to simplify the comparison between clusters. Each has a different NifA sequence, so the ability to cross-induce the gene clusters was tested using a fluorescent reporter (Supplementary Figs. 15 and 16). The *P. stuzeri* NifA was selected and used to build a genome-encoded controller using the IPTG sensor and an RBS selected to maximize the dynamic range (Supplementary Fig. 1). The induction of all three *nifH* promoters is shown in Fig. 5c and the induction of nitrogenase activity in Fig. 5d.

The native *P. stutzeri* and *A. vinelandii* clusters were strongly repressed by ammonium—the activity of the clusters was eliminated or reduced by 85%, respectively, in the presence of 17.1 mM ammonium acetate (Fig. 5e and Extended Data Fig. 7). In contrast, the inducible clusters showed little reduction in activity and the inducible *A. vinelandii* cluster exhibited almost no ammonium repression.

The inducible *nif* clusters were then tested for oxygen sensitivity. The controller is able to induce all three *nifH* promoters in the presence of oxygen (Extended Data Fig. 8). The tolerance to oxygen in the headspace was then assessed (see Methods). The native and inducible clusters were found to have the same oxygen response (Fig. 5f). The *nif* cluster from *K. oxytoca* was the most sensitive, generating the highest activity under anaerobic conditions but this was quickly abolished in the presence of oxygen. In contrast, the *nif* clusters from *P. stutzeri* and *A. vinelandii* showed a wider tolerance with optima at 1% and 0.5%, respectively. Wild-type *A. vinelandii* is able to fix nitrogen under ambient conditions due to genetic factors

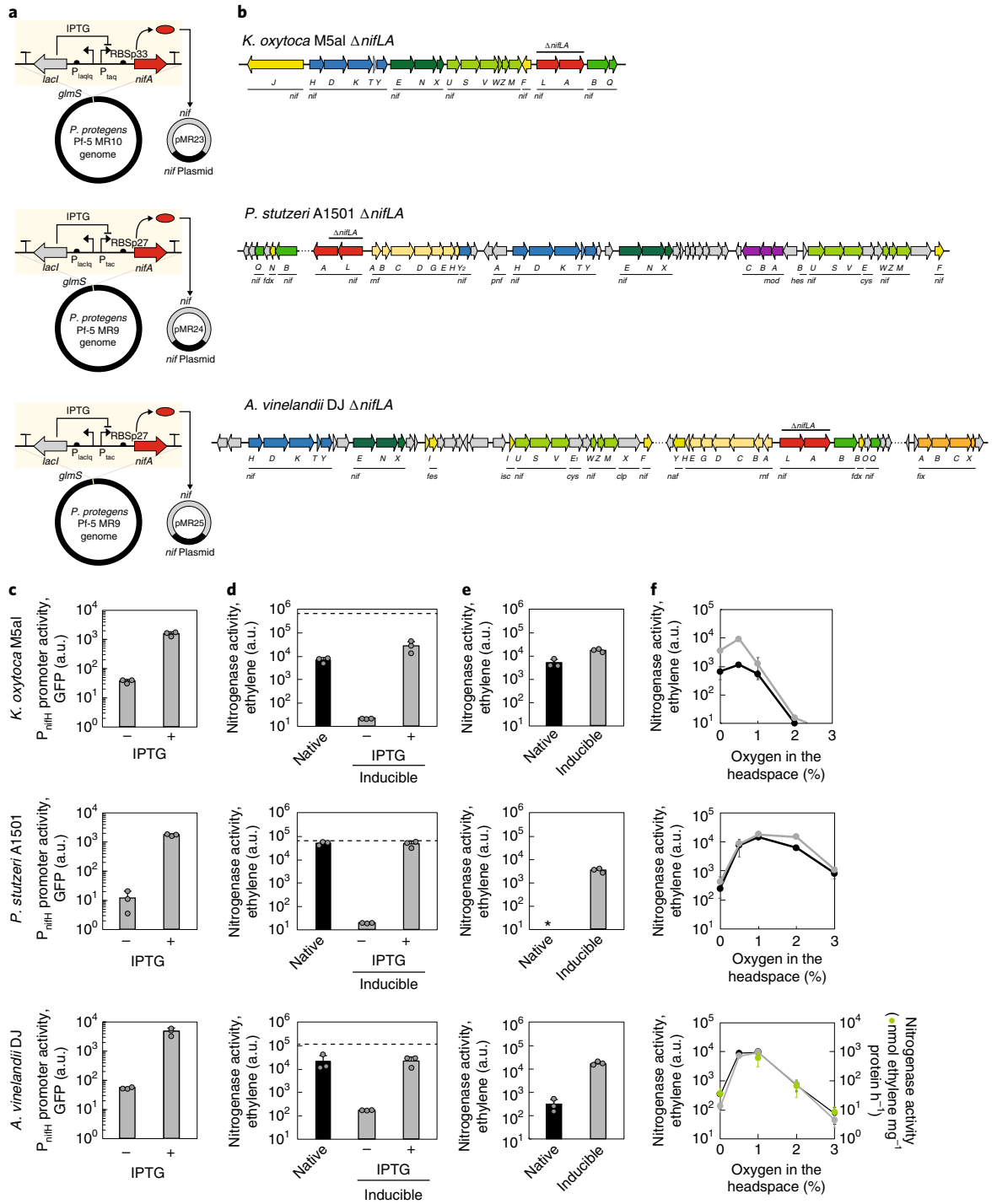

Fig. 5 | Nitrogenase activity of the inducible *nif* clusters in *P. protegens* Pf-5. a, The controllers, based on *P. stutzeri* NifA, were used for all three clusters. The plasmids and genetic parts are provided in Supplementary Tables 3 and 4. **b**, Schematics of the *nif* clusters from *K. oxytoca* (top), *P. stutzeri* (middle) and *A. vinelandii* (bottom). The deleted regions encoding the NifLA regulators are marked and their corresponding genomic locations are provided in Supplementary Table 3. The dotted lines indicate that multiple regions from the genome were cloned and combined to form the *nif* cluster. The clusters were carried on the plasmids pMR23–25 (Supplementary Table 3). **c**, Induction of the *nifH* promoters from each species by the controller (+, 0.5 mM IPTG; see Methods). **d**, Nitrogenase activities of the native cluster (intact *nifLA*) compared with the inducible clusters in the presence and absence of 0.5 mM IPTG. The dashed lines indicate the activity of the native clusters in the wild-type context. **e**, Comparisons of the sensitivity of the native and inducible (+0.5 mM IPTG) *nif* clusters to 17.1 mM ammonium acetate. The asterisk indicates ethylene production at levels below the detection limit. **f**, Nitrogenase activity as a function of the oxygen concentration in the headspace (see Methods). Comparison of the native *nif* cluster (black) to the inducible version encoding the controller with 0.5 mM IPTG induction (grey). The specific nitrogenase activity of the inducible *A. vinelandii nif* cluster is shown in green (bottom). The error bars represent the s.d. from three independent experiments performed on different days. **c**–**f**, Top, *K. oxytoca* M5al; middle, *P. stutzeri* A1501 and bottom, *A. vinelandii* DJ.

internal and external to the cluster[51,169–171]. We explored the impact of including various electron transport chains and found that *rnf1* is essential, whereas *rnf2*/*fix* had no effect (Extended Data Fig. 9). This suggests that the *rnf1* operon is the sole source of electrons in *P. protegens* Pf-5 and the Fix complex cannot compensate the Rnf complex, in contrast to what was shown in *A. vinelandii*[172].

Control of nitrogen fixation with agriculturally relevant sensors. Controllers simplify the process by which the regulation controlling a gene cluster can be changed. This can be demonstrated by placing the various strains of inducible *nif* we created under the control of 11 sensors that respond to a variety of chemicals relevant to the rhizosphere (Fig. 6). Sensors could respond to biocontrol agents or components of added fertilizer and other treatments (DAPG)[101–103]. Proximity to the plant could be detected by root exudates, including sugars (arabinose), hormones (salicylic acid), flavonoids (naringenin), antimicrobials (vanillic acid) and chemicals (cuminic acid) that remodel the microbial community[9,38–40,104–113,173–179]. Other bacteria colonizing the cereal root surface, including exogenously added plant growth promoting bacteria, release chemicals (3,4-dihydroxybenzoic acid (DHBA), 3OC6HSL and 3OC14HSL)[180–189]. Sensors that respond to these signals have been previously shown to turn on expression in bacteria that are close to the roots[114,190]. Finally, plants could also be genetically modified to excrete a non-natural chemical signal (opines) that is received by engineered bacteria[115,116]. To this end, pathways have been previously introduced into plants that lead to the secretion of opines, phloroglucinol and rhizopine[191–195].

Sensors for chemicals representative of these categories were used to construct controllers for each species. For *E. coli*, we used a 'Marionette' strain[196], which includes sensors for vanillic acid, DHBA, cuminic acid, 3OC6HSL and 3OC14HSL in the genome. The output promoter of each sensor was used to express T7 RNAP and this was found to induce the v2.1 cluster (Fig. 6c,d and Extended Data Fig. 10). For *P. protegens* Pf-5, the arabinose and naringenin sensors were used to express NifA, which led to the induction of the *nifH* promoter and nitrogenase activity (Fig. 6c,d). For *R.* sp. IRBG74, the DAPG sensor was used to drive T7 RNAP and this induced nitrogenase from the v3.2 cluster, albeit only weakly (Fig. 6c,d). For *A. caulinodans*, the salicylic acid sensor designed for *Rhizobium* was used to control NifA$^{L94Q/D95Q}$/RpoN expression and this led to a 1,000-fold induction of nitrogenase activity (Fig. 6b–d).

Plants could be engineered to release an orthogonal chemical signal that could then be sensed by a corresponding engineered bacterium[4,105]. This would have the benefit of only inducing nitrogenase in the presence of the engineered crop. To this end, legumes and *Arabidopsis* have been engineered to produce opines, including nopaline and octopine[194,195]. This has been shown to lead to the production of up to millimolar concentrations of octopine from the transgenic *Arabidopsis* lines under hydroponic culture conditions[195]. We constructed sensors for these two opines for *A. caulinodans* based on the LysR-type transcriptional activators OccR (octopine) and NocR (nopaline) and their corresponding P_{occ} and P_{noc} promoters (Fig. 6b). These sensors were connected to the expression of *nifA*$^{L94Q/D95Q}$/*rpoN* and the response from P_{nifH} was measured using a fluorescent reporter (Supplementary Fig. 18). Both response functions had a large dynamic range (Fig. 6c) and produced highly inducible nitrogenase activity (Fig. 6d,e).

Discussion

This work provides a comparison of diverse species, natural *nif* clusters, and engineering strategies (Supplementary Fig. 19), which can be used towards designing a bacterium that can deliver fixed nitrogen to a cereal crop. The goal was to obtain inducible nitrogenase activity in a strain that can associate with cereals as an endophyte or epiphyte. Different approaches were taken to make these *nif* clusters inducible, from bioinformatics and protein engineering to complete genetic reconstruction from the ground up (refactoring). In addition to the highest activity, it is essential that nitrogen fixation be robust to added nitrogenous fertilizer and micro-aerobic environments. Our most promising endophyte is a variant of *A. caulinodans* where *nifA* is knocked out of the genome and a NifA mutant and RpoN are complemented on a plasmid. For the epiphyte *P. protegens* Pf-5, the most versatile strain is based on the transfer of the *A. vinelandii nif* cluster and placement of *nifA* of *P. stutzeri* under inducible control. In both cases, nitrogenases activities equivalent to the best natural nitrogen fixers are obtained, neither show ammonium repression and optimal activity occurs at approximately 1% oxygen. Using these strains, nitrogenase can be placed under inducible control in response to cereal-root exudates (arabinose and salicylic acid), phytohormones and putative signalling molecules that could be released by genetically modified plants (nopaline and octopine).

RNA sequencing and ribosome profiling are used to debug the performances of natural and engineered *nif* clusters. The latter technique is a powerful tool in genetic engineering to infer expression levels without proteomics, identify translation errors and quantify translational parts (for example, RBSs). In this work, we used these techniques to compare the function of *nif* parts in their native and new hosts. Interestingly, the native *K. oxytoca nif* cluster performs similarly when transferred, but the refactored cluster that uses codon optimization and disrupts operons and translational coupling yielded widely varying levels of expression between genes. This could be recovered by maintaining the native operon structure in the v3.2 refactored cluster. Maintenance of the relative synthesis rates of members of an operon is one of their hypothesized functions[137,157,159]. Thus, disrupting operons and translational coupling does not impact their function in their native host[72] but impacts activity after transfer.

This work is the first step towards building strains that can efficiently deliver fixed nitrogen to cereals[4,105]. Fully realizing the goal of engineering microbial delivery to a cereal crop will require significant additional genetic engineering to maximize the ability of the microorganism to catabolize carbon sources from the plant and

Fig. 6 | Control of nitrogenase activity with sensors that respond to diverse chemicals in the rhizosphere. a, Schematic showing the origins of the chemicals. Introduced DNA, genetic modification of the plant to produce nopaline and octopine. GMO, genetically modified organism. **b**, Genetic sensors built for controlling nitrogenase activity in *A. caulinodans*. The sequences for the genetic parts are provided in Supplementary Table 4. **c**, Response functions of the sensors. Either the sensor expresses T7 RNAP, which then activates P_{T7}, or it expresses *nifA*/(*rpoN*) and activates the *nifH* promoter (the species origin is indicated in parentheses). **d**, The nitrogenase activity was measured in the presence or absence of inducer (see Methods). The refactored *K. oxytoca nif* clusters v2.1 and v3.2 were used in *E. coli* MG1655 and *R.* sp. IRBG74, respectively. The inducible *A. vinelandii nif* cluster was used in *P. protegens* Pf-5. The controller containing *nifA*/*rpoN* was used in *A. caulinodans* Δ*nifA*. **e**, Incorporation of ^{15}N into cell biomass. Nitrogen fixation in the wild-type *A. caulinodans* ORS571, *A. caulinodans* Δ*nifA* and *A. caulinodans* Δ*nifA* carrying the controller, in which *nifA*/*rpoN* is inducible by octopine (+1 mM octopine), was traced using $^{15}N_2$ and analysed using isotope-ratio mass spectrometry (see Methods). The asterisk indicates ^{15}N incorporation at levels below the detection limit. The inducers were used at the following concentrations: 50 μM vanillic acid, 500 μM DHBA, 50 μM cuminic acid, 25 nM 3OC6HSL, 500 nM 3OC14HSL, 33 μM arabinose, 100 μM naringenin, 100 nM DAPG, 200 μM salicylic acid, 1 mM nopaline and 1 mM octopine. The error bars represent the s.d. from three (**d**) or two (**e**) independent experiments performed on different days.

increase the flux of fixed-nitrogen delivery by redirecting metabolism, introducing transporters and the optimization of electron transfer. An intriguing possibility is to also genetically engineer the plant to produce orthogonal carbon sources[117,195], such as opines or less common sugars, and then place the corresponding catabolism pathways into the bacterium to create a synthetic symbiosis.

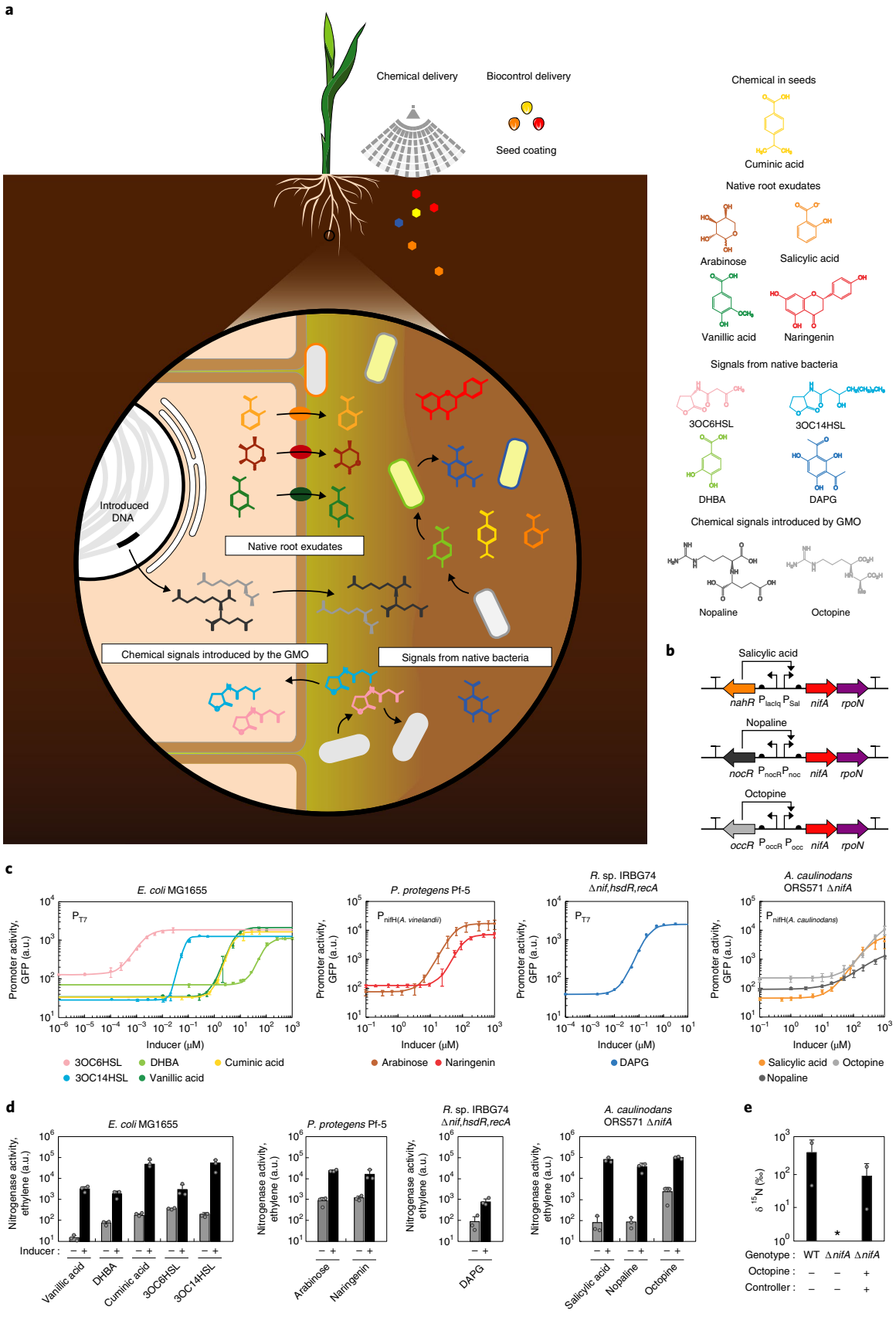

Methods

Bacterial strains and growth media. All bacterial strains and their derivatives, which were used in this study are listed in Supplementary Table 2. *E. coli* DH10-beta (New England Biolabs, cat. no. C3019) was used for cloning. *E. coli* K-12 MG1655 was used for the nitrogenase assay. *P. protegens* Pf-5 was obtained from the American Type Culture Collection (ATCC; BAA-477). For rich media, LB medium (10 g l^{-1} tryptone, 5 g l^{-1} yeast extract and 10 g l^{-1} NaCl), LB-Lennox medium (10 g l^{-1} tryptone, 5 g l^{-1} yeast extract and 5 g l^{-1} NaCl) and TY medium (5 g l^{-1} tryptone, 3 g l^{-1} yeast extract and 0.87 g l^{-1}l $CaCl_2{\cdot}2H_2O$) were used. For minimal media, BB medium (0.25 g l^{-1} $MgSO_4{\cdot}7H_2O$, 1 g l^{-1} NaCl, 0.1 g l^{-1} $CaCl_2{\cdot}2H_2O$, 2.9 mg l^{-1} $FeCl_3$, 0.25 mg l^{-1} $Na_2MoO_4{\cdot}2H_2O$, 1.32 g l^{-1} $NH_4CH_3CO_2$, 25 g l^{-1} Na_2HPO_4 and 3 g l^{-1} KH_2PO_4, pH 7.4), UMS medium[197] (0.5 g l^{-1} $MgSO_4{\cdot}7H_2O$, 0.2 g l^{-1} NaCl, 0.375 mg l^{-1} EDTA–Na_2, 0.16 $ZnSO_4{\cdot}7H_2O$, 0.2 mg l^{-1} $Na_2MoO_4{\cdot}2H_2O$, 0.25 mg l^{-1} H_3BO_3, 0.2 mg l^{-1} $MnSO_4{\cdot}H_2O$, 0.02 mg l^{-1} $CuSO_4{\cdot}5H_2O$, 1 mg l^{-1} $CoCl_2{\cdot}6H_2O$, 75 mg l^{-1} $CaCl_2{\cdot}2H_2O$, 12 mg l^{-1} $FeSO_4{\cdot}7H_2O$, 1 mg l^{-1} thiamine hydrochloride 2 mg l^{-1} D-pantothenic acid hemicalcium salt, 0.1 mg l^{-1} biotin, 4 mg l^{-1} nicotinic acid, 87.4 mg l^{-1} K_2HPO and 4.19 g l^{-1} MOPS, pH 7.0) and Burk medium[198] (0.2 g l^{-1} $MgSO_4{\cdot}7H_2O$, 73 mg l^{-1} $CaCl_2{\cdot}2H_2O$, 5.4 mg l^{-1} $FeCl_3{\cdot}6H_2O$, 4.2 mg l^{-1} $Na_2MoO_4{\cdot}2H_2O$, 0.2 g l^{-1} KH_2PO_4 and 0.8 g l^{-1} K_2HPO_4, pH 7.4) were used. The *E. coli* and *Pseudomonas* strains were incubated at 30 °C in BB minimal media. However, no growth was observed for *R.* sp. IRBG74 under these conditions. Different media and carbon sources were tested and we found that UMS media with dicarboxylic acids (malate or succinate), the major carbon source from plants[199], with 10 mM sucrose yielded the highest growth rates (Supplementary Fig. 20). Antibiotics were used at the following concentrations (μg ml^{-1}): *E. coli* (kanamycin, 50; spectinomycin, 100; tetracycline, 15; gentamicin, 15), *P. protegens* Pf-5 (kanamycin, 30; tetracycline, 50; gentamicin, 15; carbenicillin, 50), *R.* sp. IRBG74 (neomycin, 150; gentamicin, 150; tetracycline, 10; nitrofurantoin, 10) and *A. caulinodans* (kanamycin, 30; gentamicin, 15; tetracycline, 10; nitrofurantoin, 10). The chemicals, including inducers, used in this study are listed in Supplementary Table 6.

Strain construction. A *sacB* markerless insertion method was utilized to allow deletions and replacements of a native locus with synthetic parts by homologous recombination. To increase transformation efficiency in *R.* sp. IRBG74, a type-I restriction-modification system was inactivated by deleting *hsdR*, which encodes a restriction enzyme for foreign DNA[200]. Two homology arms of approximately 500 bp flanking the *hsdR* gene were amplified by PCR and cloned to yield a suicide plasmid, pMR44. The suicide plasmid was mobilized into *R.* sp. IRBG74 by triparental mating. Single-crossover recombinants were selected for resistance to gentamicin and subsequently cultured and plated on LB plates supplemented with 15% sucrose to induce deletion of the vector DNA part containing the counter-selective marker *sacB*, which converts sucrose into a toxic product (levan). Two native *nif* gene clusters encompassing *nifHDKENX* (genomic location 219,579–227,127) and *nifSW–fixABCX–nifAB–fdxN–nifTZ* (genomic location 234,635–234,802) of *R.* sp. IRBG74 were sequentially deleted using pMR45–46 (Extended Data Fig. 1). The *recA* gene was deleted using the plasmid pMR47 to increase genetic stability[201]. The *R.* sp. IRBG74 Δ*nif*, *hsdR*, *recA* strain was the basis for all experiments, unless indicated otherwise. Two homology arms of approximately 900 bp flanking the *nifA* gene were amplified by PCR and cloned to yield a suicide plasmid, pMR47, to generate *nifA* deletion in *A. caulinodans* ORS571. The suicide plasmid pMR47 in *E. coli* was mobilized into *A. caulinodans* by triparental mating. Single-crossover recombinants were selected for resistance to gentamicin, and subsequently cultured and plated on TY plates supplemented with 15% sucrose to induce deletion of the vector DNA part. All markerless deletions were confirmed by gentamicin sensitivity and diagnostic PCR. A list of the mutant strains is provided in Supplementary Table 2.

Plasmid system. Plasmids with the pBBR1 origin were derived from pMQ131 and pMQ132 (ref. [133]). Plasmids with the pRO1600 origin were derived from pMQ80 (ref. [133]). Plasmids with the RK2 origin were derived from pJP2 (ref. [202]). Plasmids with the RSF1010 origin were derived from pSEVA651 (ref. [203]). Plasmids with the IncW origin were derived from pKT249 (ref. [71]). The plasmids used in this study are provided in Supplementary Table 3.

Phylogenetic analysis of *nif* clusters. Phylogenetic analysis was performed based on full-length 16S ribosomal RNA gene sequences (*K. oxytoca* M5al, BWI76_05380; *A. vinelandii* DJ, Avin_55000; *R. sphaeroides* 2.4.1, DQL45_00005; *Cyanothece* ATCC51142, cce_RNA045; *Azospirillum brasilense* Sp7, AMK58_25190; *R. palustris* CGA009, RNA_55; *P. protegens* Pf-5, PST_0759; *Paenibacillus polymyxa* WLY78, JQ003557). A multiple sequence alignment was generated using MUSCLE[204]. A phylogenetic tree was constructed using the Geneious software (R9.0.5) with the Jukes–Cantor distance model and UPGMA as a tree build method, with bootstrap values from 1,000 replicates.

Construction of *nif* clusters. Each cluster was amplified from genomic DNA as multiple fragments using PCR and assembled with the plasmid backbone using yeast assembly. The clusters were cloned into different plasmid systems to facilitate transfer. The broad-host-range plasmid based on a pBBR1 origin was used for transfers to *E. coli* and *R.* sp. IRBG74. In addition, a second RK2-origin plasmid compatible with the pBBR1 origin plasmid was used for the *nif* cluster from *A. caulinodans* ORS571, which includes two *nifH* homologs (Supplementary Fig. 1). These plasmids contain the RK2 origin of transfer (*oriT*) to enable the conjugative transfer of large DNA. For transfer to *P. protegens* Pf-5, this plasmid system was found to be unstable and produce a mixed population (Supplementary Fig. 21). The *Pseudomonas*-specific plasmid based on pRO1600 origin with the *oriT* was used to transfer into this strain. To obtain large *nif* clusters on mobilizable plasmids, the genomic DNAs from *K. oxytoca*, *P. stutzeri*, *A. vinelandii*, *A. caulinodans* and *R. sphaeroides* were purified using the Wizard genomic DNA purification kit, following the isolation protocol for Gram-negative bacteria (Promega, cat. no. A1120). Genomic DNA from *Cyanothece* ATCC51142, *A. brasilense* ATCC29729, *R. palustris* ATCC BAA-98 and *G. diazotrophicus* ATCC49037 were obtained from the ATCC. Each *nif* cluster was amplified into several fragments (4–10 kb) with 45-bp upstream and downstream linkers at the 5′ and 3′-most end of the cluster using PCR (with the primer sets listed in Supplementary Table 1) and assembled onto the linearized *E. coli*–yeast shuttle vectors pMR1 for *E. coli* and rhizobia, and pMR2 for *P. protegens* Pf-5 using yeast recombineering[133]. For the *nif* cluster of *P. polymyxa* WLY78, the DNA-sequence information were gleaned from contig ALJV01 (ref. [70]) and the DNA of the *nif* cluster was synthesized de novo into four fragments using GeneArt gene synthesis (Thermo Fisher Scientific), which were used as templates for PCR amplification and assembly. The amplified fragments from two to eight DNA fragments (Supplementary Table 1) were assembled with a linearized vector into a single large plasmid using a one-pot yeast assembly procedure[133]. Once assembled, the *nif* cluster plasmids were isolated from yeast using a Zymoprep yeast miniprep kit (Zymo Research, cat. no. D2004) and transformed into *E. coli*. The purified plasmid was isolated from *E. coli* and sequenced to verify the correct assembly and sequences (MGH CCIB DNA Core facility). *E. coli* containing a mutation-free plasmid were stored for further experiments. The precise genomic locations of all of the *nif* clusters are provided in Supplementary Table 1, and the plasmids containing *nif* clusters are provided in Supplementary Table 3 and their sequences are provided in Supplementary Files. For the *P. stutzeri* A1501 *nif* cluster, as neither the published strain nor its sequence have been made available by the authors, it is impossible to perfectly replicate the strain and differences in the cluster boundary or mutations to the regulation during construction[66,205], which could explain the discrepancy in the ammonium sensitivity of nitrogenase.

Construction of refactored *nif* v3.2. The six transcriptional units (*nifHDKTY*, *nifENX*, *nifJ*, *nifBQ*, *nifF* and *nifUSVWZM*) were amplified from the plasmid pMR3, which harbours the native *K. oxytoca nif* cluster. Each unit was divided onto six level-1 module plasmids, where the *nif* genes were preceded by a terminator. The T7 promoter wild-type P_{WT} or T7 promoter variant P_2 was placed between a terminator and the first gene of the transcriptional unit. Assembly linkers (approximately 45 bp) were placed at both ends of the units. The level-1 plasmids (pMR32–37) are provided in Supplementary Table 3. Each of the six plasmids were linearized by digestion with restriction enzymes and assembled with linearized pMR1 or pMR2 vectors into a single large plasmid using a one-pot yeast assembly procedure[133], yielding pMR38 and pMR39.

Transformation. Electroporation was used to transfer plasmids into *P. protegens* Pf-5. A single colony was inoculated into 4 ml LB medium and incubated for 16 h at 30 °C with shaking at 250 r.p.m. The cell pellets were washed twice with 2 ml of 300 mM sucrose and dissolved in 100 μl of 300 mM sucrose at room temperature. A total of 50–100 ng DNA was electroporated and recovered in 1 ml LB medium for 1 h before plating on selective LB plates. Triparental mating was used to transfer DNA from *E. coli* to rhizobia. An aliquot of 40 μl donor cells in the late log phase (optical density $(OD)_{600}$ of approximately 0.6) and 40 μl helper cells in the late log phase containing pRK2013 were mixed with 200 μl recipient rhizobia cells in the late log phase (OD_{600} of approximately 0.8) and washed in 200 μl TY medium. Mating was initiated by spotting 20 μl of the mixed cells on TY plates and incubated at 30 °C for 6 h. The mating mixtures were plated on TY medium supplemented with nitrofurantoin to isolate the rhizobia transconjugants.

Genetic-part characterization for rhizobia. Promoters, RBS and terminators were characterized using a plasmid-based system (pBBR1-ori) and fluorescent reporters (GFPmut3b and mRFP1; Supplementary Tables 3 and 4). The same growth and measurement protocols were used, as follows. Single colonies were inoculated into 0.5 ml TY medium supplemented with antibiotics in 96-deep-well plates (USA Scientific, cat. no. 18962110) and incubated overnight at 30 °C and 900 r.p.m. in a Multitron incubator (Infors HT). Aliquots (1.5 μl) of the overnight cultures were diluted in 200 μl TY medium containing antibiotics and the appropriate inducers (if required) in 96-well plates (Thermo Fisher Scientific, cat. no. 12565215), and incubated for 7 h at 30 °C and 1,000 r.p.m. in an ELMI DTS-4 shaker. Aliquots (8 μl) of these cultures were then diluted in 150 μl PBS with 2 mg ml^{-1} kanamycin for analysis using flow cytometry (see below). Constitutive promoters were transcriptionally fused to a reporter gene, cultured as above and evaluated using flow cytometry (Supplementary Fig. 3a). The RBS library was designed using the RBS Library Calculator[153], using the highest-resolution mode and the 3′ 16 S rRNA

sequence 3′-ACCTCCTTC-5′ for *R.* sp. IRBG74. To determine the RBS strength, the IPTG-inducible green fluorescent protein (GFP) expression plasmid pMR40 was used (Supplementary Fig. 4a) and the cells were cultured in the presence of 1 mM IPTG. The T7 RNAP terminators were characterized by placing the terminator between two fluorescent reporters, both of which are transcribed from the same upstream T7 promoter (Supplementary Fig. 5a)[155]. A stronger terminator leads to lower expression of the second reporter. The terminator-containing plasmids were transformed into the MR22 strain, where T7 RNAP is under IPTG control, and the cells were cultured in the presence of 1 mM IPTG (Supplementary Fig. 5a). The terminator strength (T_s) was calculated by dividing the fluorescence measured from a construct containing the terminator by the fluorescence when the terminator was replaced with a 40-bp spacer.

Sensor characterization for rhizobia. Sensors were characterized using a plasmid-based system (pBBR1-ori) and fluorescent reporters (GFPmut3b; Supplementary Tables 3 and 4). The following combinations of cognate regulators and inducible promoters were characterized: IPTG-inducible LacI–$P_{A1lacO1}$, DAPG-inducible PhlF–P_{Phl}, aTc-inducible TetR–P_{Tet}, 3OC6HSL inducible LuxR–P_{Lux}, salicylic acid-inducible NahR–P_{Sal} and cuminic acid-inducible CymR–P_{Cym}; these systems were optimized for *R.* sp. IRBG74 (Supplementary Fig. 6). Opine-inducible OccR–P_{occ} and nopaline-inducible NocR–P_{noc} systems were optimized for *A. caulinodans* (Supplementary Fig. 12). To characterize the sensors, single colonies were inoculated into 0.5 ml TY medium supplemented with antibiotics in 96-deep-well plates and incubated overnight at 30 and 37 °C for *Rhizobium* and *Azorhizobium*, respectively, and 900 r.p.m. in a Multitron incubator. Aliquots (1.5 µl) of the overnight cultures were diluted in 200 µl TY medium containing antibiotics and the appropriate inducers in 96-well plates, and incubated for 7 h at 30 °C and 1,000 r.p.m. in an ELMI DTS-4 shaker. Aliquots (8 µl) of these cultures were then diluted in 150 µl PBS with 2 mg ml^{-1} kanamycin for analysis using flow cytometry (see below).

Genetic-part characterization for *P. protegens*. Promoters, RBS and terminators were characterized using a plasmid-based system (pRO1600-ori) and fluorescent reporters (GFPmut3b and mRFP1; Supplementary Tables 3 and 4). The same growth and measurement protocols were used, as follows. Single colonies were inoculated into 1 ml LB medium supplemented with antibiotics in 96-deep-well plates and incubated overnight at 30 °C and 900 r.p.m. in a Multitron incubator. Aliquots (0.5 µl) of the overnight cultures were diluted in 200 µl LB medium containing antibiotics and the appropriate inducers (if required) in 96-well plates, and incubated for 7 h at 30 °C and 1,000 r.p.m. in an ELMI DTS-4 shaker. Aliquots (10 µl) of these cultures were then diluted in 150 µl PBS with 2 mg ml^{-1} kanamycin for analysis using flow cytometry (see below). Constitutive promoters were transcriptionally fused to a reporter gene, cultured as above, and evaluated using flow cytometry (Supplementary Fig. 3a). The RBS library was designed using the RBS Library Calculator[153], using the highest-resolution mode and the 3′ 16 S rRNA sequence 3′-ACCTCCTTA-5′ for *P. protegens* Pf-5. The arabinose-inducible GFP-expression plasmid pMR66 was used to determine the RBS strength (Supplementary Fig. 4b), and the cells were cultured in the presence of 7 µM arabinose. The terminator-containing plasmids were transformed into the MR7 strain, where T7 RNAP is under IPTG control, and the cells were cultured in the presence of 0.5 mM IPTG (Supplementary Fig. 5b). The T_s was calculated as described earlier.

Sensor characterization for *P. protegens*. Sensors were characterized using a plasmid-based system (pRO1600-ori) and fluorescent reporters (GFPmut3b; Supplementary Tables 3 and 4). The following combinations of cognate regulators and inducible promoters were characterized: IPTG-inducible LacI–P_{tac}, DAPG-inducible PhlF–P_{Phl}, aTc-inducible TetR–P_{Tet}, 3OC6HSL inducible LuxR–P_{Lux}, arabinose-inducible AraC–P_{BAD}, cuminic acid-inducible CymR–P_{Cym} and naringenin-inducible FdeR–P_{Fde}; these systems were optimized for *P. protegens* Pf-5 (Supplementary Fig. 7). To characterize the sensors, single colonies were inoculated into 1 ml LB medium supplemented with antibiotics in 96-deep-well plates and incubated overnight at 30 °C and 900 r.p.m. in a Multitron incubator. Aliquots (0.5 µl) of the overnight cultures were diluted in 200 µl LB medium containing antibiotics and the appropriate inducers in 96-well plates, and incubated for 7 h at 30 °C and 1,000 r.p.m. in an ELMI DTS-4 shaker. Aliquots (10 µl) of these cultures were then diluted in 150 µl PBS with 2 mg ml^{-1} kanamycin for analysis using flow cytometry (see below).

Genomic integration and characterization of controllers. The mini-Tn7 insertion system[168] was used to introduce a controller into the genome of *P. protegens* Pf-5. The IPTG-inducible T7 RNAP expression system and a tetracycline-resistant marker *tetA* was placed between two Tn7 ends (Tn7L and Tn7R), yielding the controller plasmid pMR86. This was introduced into *P. protegens* Pf-5 by dual transformation with pTNS3 (ref. [168]) encoding the *TnsABCD* transposase. A genomically integrated controller located 25 bp downstream of the stop codon of *glmS* was confirmed by PCR and sequencing. A markerless insertion method using homologous recombination was employed in *R.* sp. IRBG74 (described earlier). A controller encoding an inducible T7 RNAP system flanked by two homology fragments, which enables the replacement of *recA*, was cloned into a suicide plasmid. These controller plasmids (IPTG-inducible, pMR82–84; DAPG-inducible, pMR85) in *E. coli* were mobilized into *R.* sp. IRBG74 MR18 (Δ*hsdR* Δ*nif*) by triparental mating, generating the controller strains (MR19, -20, -21 and -22, respectively). The controller integration in the genome was confirmed by gentamicin sensitivity and diagnostic PCR. The reporter plasmids pMR80 and pMR81 containing *gfpmut3b* under the control of the T7 promoter were introduced into the *P. protegens* Pf-5 and *R.* sp. IRBG74 controller strains, respectively (Extended Data Fig. 5a and Supplementary Fig. 8). The controllers were characterized using the same experimental conditions as for the sensor characterization for *P. protegens* Pf-5 and *R.* sp. IRBG74 (described earlier).

Construction and characterization of Marionette-based controllers. To regulate nitrogenase expression in the *E. coli* Marionette MG1655 strain[196], the *yfp* in the 12 reporter plasmids was replaced with T7 RNAP, while keeping other genetic parts (for example, promoters and RBSs) unchanged (Extended Data Fig. 9a). The reporter plasmid pMR123, in which *gfpmut3b* is fused to the T7 promoter variant P_2, was co-transformed to analyse the response functions of each of the 12 T7 RNAP controller plasmids (Extended Data Fig. 9b). To characterize the controllers, single colonies were inoculated into 1 ml LB medium supplemented with antibiotics in 96-deep-well plates and incubated overnight in a Multitron incubator at 30 °C and 900 r.p.m. Aliquots (0.5 µl) of the overnight cultures were diluted in 200 µl LB containing antibiotics and the appropriate inducers in 96-well plates and incubated for 6 h at 30 °C and 1,000 r.p.m. in an ELMI DTS-4 shaker. Aliquots (4 µl) of these cultures were diluted in 150 µl PBS with 2 mg ml^{-1} kanamycin for analysis by flow cytometry.

Flow cytometry. Cultures with fluorescence proteins were analysed by flow cytometry using a BD Biosciences LSRII Fortessa analyzer with a 488 nm laser and 510/20-nm band-pass filter for GFP, and a 561 nm laser and 610/20 nm band-pass filter for mCherry and mRFP1. Cells were diluted in 96-well plates containing PBS supplemented with 2 mg ml^{-1} kanamycin after incubation. The cells were collected over 20,000 events, which were gated using forward and side scatter to remove background events using FlowJo (TreeStar Inc.). The median fluorescence from the cytometry histograms was calculated for all samples. The median autofluorescence was subtracted from the median fluorescence and reported as the fluorescence value in arbitrary units.

***E. coli* and *K. oxytoca* nitrogenase assays.** Cultures were initiated by inoculating a single colony into 1 ml LB supplemented with the appropriate antibiotics in 96-deep-well plates (USA Scientific, cat. no. 18962110) and incubated overnight in a Multitron incubator at 30 °C and 900 r.p.m. Aliquots (5 µl) of the overnight cultures were diluted in 500 µl BB medium with 17.1 mM $NH_4CH_3CO_2$ and the appropriate antibiotics in 96-deep-well plates, and incubated for 24 h at 30 °C and 900 r.p.m. in a Multitron incubator. The cultures were diluted to an OD_{600} of 0.4 in 2 ml BB medium supplemented with the appropriate antibiotics, 1.43 mM serine to facilitate nitrogenase depression[206] and an inducer (if necessary) in 10-ml glass vials with PTFE-silicone septa screw caps (Supelco Analytical, cat. no. SU860103). The headspace in the vials was replaced with 100% argon gas using a vacuum manifold. Acetylene, freshly generated from CaC_2 in a Burris bottle, was injected into each culture vial to 10% (vol/vol) concentration to initiate the reaction. The acetylene reduction was carried out for 20 h at 30 °C with shaking at 250 r.p.m. in an Innova 44 shaking incubator (New Brunswick) to prevent cell aggregation, followed by quenching through the addition of 0.5 ml of 4 M NaOH to each vial.

***P. protegens* Pf-5 nitrogenase assay.** Cultures were initiated by inoculating a single colony into 1 ml LB medium supplemented with the appropriate antibiotics in 96-deep-well plates and incubated overnight at 30 °C and 900 r.p.m. in a Multitron incubator. Aliquots (5 µl) of the overnight cultures were diluted in 500 µl BB medium with 17.1 mM $NH_4CH_3CO_2$ and the appropriate antibiotics in 96-deep-well plates, and incubated in a Multitron incubator for 24 h at 30 °C and 900 r.p.m. The cultures were diluted to an OD_{600} of 0.4 in 2 ml BB medium supplemented with the appropriate antibiotics, 1.43 mM serine and an inducer (if necessary) in 10-ml glass vials with PTFE-silicone septa screw caps. The headspace in the vials was replaced with 99% argon and 1% oxygen gas (Airgas) using a vacuum manifold. Acetylene was injected into each culture vial to a concentration of 10% (vol/vol) to initiate the reaction. The acetylene reduction was carried out for 20 h at 30 °C with shaking at 250 r.p.m., followed by quenching through the addition of 0.5 ml of 4 M NaOH to each vial.

Nitrogenase assay of *Rhizobium* strains. Cultures were initiated by inoculating a single colony into 0.5 ml TY medium supplemented with the appropriate antibiotics in 96-deep-well plates and incubated overnight at 30 °C and 900 r.p.m. in a Multitron incubator. Aliquots (5 µl) of the overnight cultures were diluted in 500 µl UMS medium with 30 mM succinate, 10 mM sucrose, 10 mM NH_4Cl and the appropriate antibiotics in 96-deep-well plates, and incubated in a Multitron incubator for 24 h at 30 °C and 900 r.p.m. The cultures were diluted to an OD_{600} of 0.4 in 2 ml UMS medium plus 30 mM succinate and 10 mM sucrose supplemented with the appropriate antibiotics, 1.43 mM serine and an inducer (if necessary)

in 10-ml glass vials with PTFE-silicone septa screw caps. The headspace in the vials was replaced with 99% argon and 1% oxygen gas using a vacuum manifold. Acetylene was injected into each culture vial to a concentration of 10% (vol/vol) to initiate the reaction. The acetylene reduction was carried out for 20 h at 30 °C with shaking at 250 r.p.m., followed by quenching through the addition of 0.5 ml of 4 M NaOH to each vial.

***A. caulinodans* and *P. stutzeri* nitrogenase assays.** Cultures were initiated by inoculating a single colony into 0.2 ml TY medium supplemented with the appropriate antibiotics in 96-deep-well plates and incubated overnight at 900 r.p.m. in a Multitron incubator at 37 and 30 °C for *A. caulinodans* and *P. stutzeri*, respectively. Aliquots (5 µl) of the overnight cultures were diluted in 500 µl UMS medium with 30 mM lactate and 10 mM NH_4Cl and the appropriate antibiotics in 96-deep-well plates and incubated at 900 r.p.m. for 24 h at the appropriate temperatures in a Multitron incubator. The cultures were diluted to an OD_{600} of 0.4 in 2 ml UMS medium plus 30 mM lactate supplemented with the appropriate antibiotics and an inducer (if necessary) in 10-ml glass vials with PTFE-silicone septa screw caps. The headspace in the vials was replaced with 99% argon plus 1% oxygen gas using a vacuum manifold. Acetylene was injected into each culture vial to a concentration of 10% (vol/vol) to initiate the reaction. The acetylene reduction was carried out for 20 h at 30 °C with shaking at 250 r.p.m., followed by quenching through the addition of 0.5 ml of 4 M NaOH to each vial.

***A. vinelandii* nitrogenase assay.** Cultures were initiated by inoculating a single colony into 0.5 ml Burk medium supplemented with the appropriate antibiotics in 96-deep-well plates and incubated overnight at 30 °C and 900 r.p.m. in a Multitron incubator. Aliquots (5 µl) of the overnight cultures were diluted in 500 µl Burk medium with 17.1 mM $NH_4CH_3CO_2$ and the appropriate antibiotics in 96-deep-well plates and incubated for 24 h at 30 °C and 900 r.p.m. in a Multitron incubator. The cultures were diluted to an OD_{600} of 0.4 in 2 ml Burk medium in 10-ml glass vials with PTFE-silicone septa screw caps. The headspace in the vials was replaced with 97% argon and 3% oxygen gas (Airgas) using a vacuum manifold. Acetylene was injected into each culture vial to a concentration of 10% (vol/vol) to initiate the reaction. The acetylene reduction was carried out for 20 h at 30 °C with shaking at 250 r.p.m., followed by quenching through the addition of 0.5 ml of 4 M NaOH to each vial.

Nitrogenase activity assay at varying oxygen levels. Following an overnight incubation in minimal medium with a nitrogen source (described earlier), cultures were diluted to an OD_{600} of 0.4 in 2 ml minimal medium, 1.43 mM serine (for *E. coli* and *P. protegens* Pf-5) and an inducer (for the inducible systems) in 10-ml glass vials with PTFE-silicone septa screw caps. The vial headspace was replaced with either 100% nitrogen gas (for *E. coli*) or 99% nitrogen plus 1% oxygen (for *P. protegens* Pf-5 and *A. caulinodans*) using a vacuum manifold. The cultures were incubated for 6 h and 9 h for *P. protegens* Pf-5 and *A. caulinodans*, respectively, at 30 °C and 250 r.p.m., after which the oxygen concentrations in the headspace were recorded with the optical oxygen meter FireStingO2 equipped with a needle-type sensor OXF500PT (Pyro Science). After the induction period, the headspace in the vials was replaced with 100% argon. The initial oxygen levels in the headspace were adjusted by injecting pure oxygen via a syringe into the headspace of the vials and stabilized with shaking at 250 r.p.m. at 30 °C for 15 min, followed by the injection of acetylene to a concentration of 10% (vol/vol) into each culture vial to initiate the reaction and the initial oxygen concentrations in the headspace were recorded concomitantly. The oxygen levels in the headspace were maintained around the setting points (below ±0.25% O_2), while incubating at 250 r.p.m. and 30 °C, by injecting oxygen every hour for 3 h with oxygen monitoring before and after the oxygen spiking (Supplementary Fig. 14). The reactions were quenched after 3 h of incubation through the injection of 0.5 ml of 4 M NaOH to each vial using a syringe.

Nitrogenase activity assay in the presence of ammonium. Following an overnight incubation in minimal medium with a nitrogen source (described above), cultures were diluted to an OD_{600} of 0.4 in 2 ml ammonium-free minimal media, 1.43 mM serine (for *E. coli* and *P. protegens* Pf-5) and an inducer (for the inducible systems) in 10-ml glass vials with PTFE-silicone septa screw caps. Ammonium (17.1 mM $NH_4CH_3CO_2$ for *E. coli* and *P. protegens* Pf-5, and 10 mM NH_4Cl for the rhizobia strains) was added to the ammonium-free minimal media when testing the ammonium tolerance of the nitrogenase activity. The headspace in the vials was replaced with either 100% argon gas (for *E. coli*) or 99% argon plus 1% oxygen (for the *Pseudomonas* and *Rhizobia* strains) using a vacuum manifold. Acetylene was injected into each culture vial to a concentration of 10% (vol/vol) to initiate the reaction. The acetylene reduction was carried out for 20 h at 30 °C with shaking at 250 r.p.m., followed by quenching through the addition of 0.5 ml of 4 M NaOH to each vial.

Ethylene quantification. Ethylene production was analysed by gas chromatography using an Agilent 7890A GC system (Agilent Technologies, Inc.) equipped with a PAL headspace autosampler and flame ionization detector as follows. An aliquot of 0.5 ml headspace pre-incubated to 35 °C for 30 s was injected and separated for 4 min on a GS-CarbonPLOT column (0.32 mm × 30 m, 3 µm; Agilent) at 60 °C and a He flow rate of 1.8 ml min^{-1}. Detection occurred in a flame ionization detector heated to 300 °C with a gas flow of 35 ml min^{-1} H_2 and 400 ml min^{-1} air. Acetylene and ethylene were detected at 3.0 and 3.7 min after injection, respectively. Ethylene production was quantified by integrating the 3.7 min peak using the Agilent GC/MSD ChemStation software and converted to the molar concentration of ethylene.

Specific nitrogenase activity of *A. caulinodans* and *P. protegens* Pf-5. Following an overnight incubation in minimal medium with a nitrogen source (described earlier), cultures were diluted to an OD_{600} of 0.4 in 2 ml minimal medium, 1.43 mM serine (for *P. protegens* Pf-5) and an inducer (for the inducible systems) in the absence or presence of ammonium (17.1 mM ammonium acetate and 10 mM ammonium chloride for *P. protegens* Pf-5 and *A. caulinodans*, respectively) in 10-ml glass vials with PTFE-silicone septa screw caps. Two replicates were carried out for each culture condition. The vial headspace was replaced with 99% argon plus 1% oxygen using a vacuum manifold. The cultures were incubated for 6 h and 9 h for *P. protegens* Pf-5 and *A. caulinodans*, respectively, at 30 °C and 250 r.p.m. The oxygen concentrations were maintained around the setting points during incubation at 250 r.p.m. and 30 °C for 3 h (described earlier). One of the replicates was chilled on ice and pelleted by centrifugation for protein quantification, and the other replicate was injected with 0.5 ml of 4 M NaOH to stop the reaction for ethylene quantification after the 3 h incubation. The protein concentrations of the cell lysates were quantified using a Bradford assay (Bio-Rad, cat. no. 5000002).

***A. caulinodans* ^{15}N-incorporation assay.** Cultures were initiated by inoculating a single colony into 5 ml TY medium supplemented with the appropriate antibiotics in 15-ml culture tubes and incubated overnight at 250 r.p.m. and 30 °C in an Excella E25 incubator (Eppendorf). Aliquots (1 ml) of the overnight cultures were diluted in 20 ml UMS medium with 30 mM lactate, 10 mM NH_4Cl and the appropriate antibiotics in 125-ml Erlenmeyer flasks, and incubated for 24 h in an Excella E25 incubator at 200 r.p.m. and 30 °C. The cultures were diluted to an OD_{600} of 0.4 in 25 ml UMS medium plus 30 mM lactate supplemented with the appropriate antibiotics and an inducer (if necessary) in 125-ml Erlenmeyer flasks with rubber stoppers. A 10-ml volume of gas in the headspace was removed and 10 ml $^{15}N_2$ gas ($^{15}N_2$ atom 98%; Sigma-Aldrich, cat. no. 364584) was injected. $^{15}N_2$ incorporation was carried for 24 h at 30 °C with shaking at 200 r.p.m., after which the cultures were collected by centrifugation, frozen and stored at −20 °C. The cell pellets were freeze-dried and the $^{15}N/^{14}N$ ratio was analysed at the UW-Madison Soil Science Facility using isotope-ratio mass spectrometry.

Growth assay in ammonium-free agar slopes. Glycerol stocks of the *A. caulinodans* strains were streaked on a TY plate and incubated at 37 °C for 2 d. Agar slopes were prepared by adding 0.6% (w/v) agarose (Melford, cat. no. A20090–50.0) into ammonium-free UMS medium with 20 mM succinate, which was sterilized by autoclaving at 121 °C for 30 min. UMS agarose medium (10 ml) supplemented with antibiotics and 1 mM IPTG (if necessary) was added into 28-ml glass vials with screw-cap lids with rubber inserts (Thermo Fischer Scientific, cat. no. 14803572) and cooled before inoculation. Single colonies were streaked on agarose slopes, the headspace in the vials was equilibrated at 3% oxygen and 97% nitrogen for 30 min in a dry anaerobic glove box (Belle Technology) and sealed. The vials were incubated at 37 °C for 40 h. The cell cultures on the agarose slopes were resuspended in 1 ml water and growth was measured by OD at 600 nm.

Sample preparation for RNA-seq and ribosome profiling. Cultures of *K. oxytoca*, *E. coli*, *P. protegens* Pf-5 and *R.* sp. IRBG74 were cultured following the same protocol as that for the nitrogenase activity assays (described earlier) with a few changes. Following an overnight incubation in minimal medium with a nitrogen source, the cultures were diluted to an OD_{600} of 0.4 in 25 ml minimal medium (with an inducer, if needed) and antibiotics in 125-ml Wheaton serum vials (DWK Life Sciences, cat. no. 223748) with septum stoppers (Thermo Fisher Scientific, cat. no. FB57873). The vial headspace was replaced with either 100% nitrogen gas (for *E. coli* and *K. oxytoca*) or 99% nitrogen plus 1% oxygen (for *P. protegens* Pf-5 and *R.* sp. IRBG74) using a vacuum manifold. The cultures were incubated for 6 h at 30 °C and 250 r.p.m., and then rapidly filtered onto a nitrocellulose filter with a 0.45-µM pore size (Thermo Fisher Scientific, cat. no. GVS1215305). The cell pellets from three vials were combined using a stainless-steel scoopula (Thermo Fisher Scientific, cat. no.14-357Q) and then flash-frozen in liquid nitrogen. The frozen pellets were added to 650 µl of frozen droplets of lysis buffer (20 mM Tris (pH 8.0), 100 mM NH_4Cl, 10 mM $MgCl_2$, 0.4% Triton X-100, 0.1% Tergitol, 1 mM chloramphenicol and 100 U ml^{-1} DNase I) in a pre-chilled 25 ml canister (Retsch, cat. no. 014620213) in liquid nitrogen and pulverized five times for 3 min with intermittent cooling between cycles using a TissueLyser II (Qiagen) set at 15 Hz. The pellet was removed by centrifugation at 20,000 r.c.f. for 10 min at 4 °C and the lysate was recovered in the supernatant.

RNA-seq experiments. The RNA-seq and ribosome-footprint profiling were carried out according to the method described earlier with a few modifications[135,137]. Total RNA was isolated using the hot phenol–SDS extraction

method[207]. The rRNA fractions were subtracted from the total using the MICROBExpress kit (Thermo Fisher Scientific, cat. no. AM1905). The remaining mRNAs and transfer RNAs were fragmented using RNA fragmentation reagents (Invitrogen) at 95 °C for 1 m 45 s. The RNA fragments (10–45 bp) were isolated from a 15% TBE–urea polyacrylamide gel (Thermo Fisher Scientific, cat. no. EC6885). The 3′ ends of the RNA fragments were dephosphorylated using 20 U T4 polynucleotide kinase (New England Biolabs) in a 20-µl reaction volume supplemented with 20 U SUPERase·In (Invitrogen) at 37 °C for 1 h, after which the denatured fragments (5 pmol) were incubated at 80 °C for 2 min and ligated to 1 µg of the oligo (/5rApp/CTGTAGGCACCATCAAT/3ddc/; Integrated DNA Technologies) in a 20-µl reaction volume supplemented with 8 µl of 50% PEG 8000, 2 µl 10×T4 RNA ligase 2 buffer, 1 µl of 200 U µl^{-1} truncated K277Q T4 ligase 2 (New England Biolabs, cat. no. M0351) and 1 µl of 20 U µl^{-1} SUPERase·In at 25 °C for 3 h. The ligated fragments (35–65 bp) were isolated from a 10% TBE–urea polyacrylamide gel (Thermo Fisher Scientific, cat. no. EC6875). Complementary DNA libraries from the purified mRNA products were reverse-transcribed using Superscript III (Invitrogen, cat. no. 18080044) with the oCJ485 primer (/5Phos/AGATCGGAAGAGCGTCGTGTAGGGAAAGAGTGT/iSp18/CAAGCAGAAGACGGCATACGAGATATTGATGGTGCCTACAG) at 50 °C for 30 min and the RNA products were subsequently hydrolysed by the addition of NaOH to a final concentration of 0.1 M, followed by incubation at 95 °C for 15 min. The cDNA libraries (125–150 bp) were isolated from a 10% TBE–urea polyacrylamide gel (Thermo Fisher Scientific, cat. no. EC6875). The cDNA products were circularized in a 20-µl reaction volume supplemented with 2 µl 10×CircLigase buffer, 1 µl of 1 mM ATP, 1 µl of 50 mM $MnCl_2$ and 1 µl CircLigase (Epicenter) at 60 °C for 2 h and heat inactivated at 80 °C for 10 min. The circularized DNA (5 µl) was amplified using Phusion HF DNA polymerase (New England Biolabs) with the o231 primer (CAAGCAGAAGACGGCATACGA) and indexing primers (AATGATACGGCGACCACCGAGATCTACACGATCGGAAGAGCACACGTCTGAACTCCAGTCACNNNNNNACACTCTTTCCCTACAC) for 7–10 cycles. The amplified products (125–150 bp) were recovered from an 8% TBE–urea polyacrylamide gel (Thermo Fisher Scientific, cat. no. EC62152). The purified products were analysed using a BioAnalyzer (Agilent) and sequenced using a sequencing primer (CGACAGGTTCAGAGTTCTACAGTCCGACGATC) and an Illumina HiSeq 2500 in rapid-run mode. To generate the RNA-seq read profile for each *nif* cluster, the raw trace profiles were multiplied by 10^7 and normalized to the respective total reads from the coding sequences of each species (*K. oxytoca* M5al, CP020657.1; *E. coli* MG1655, NC_000913.3; *P. protegens* Pf-5, CP000076; *R.* sp. IRBG74 HG518322, HG518323, HG518324 and an appropriate plasmid carrying a *nif* cluster). The mRNA expression levels of each gene were estimated using the total sequencing reads mapped onto the gene, representing fragments per kilobase of transcript per million fragments mapped units (FPKM).

Ribosome-profiling experiments. RNA was diluted to 0.5 mg in 200 µl of the lysis buffer including 5 mM $CaCl_2$, 100 U SUPERase·In (Invitrogen) and 15 U micrococcal nuclease (Roche) and incubated at 25 °C for 1 h to obtain ribosome-protected monosomes. The digestions were quenched by the addition of EGTA to a final concentration of 6 mM and then kept on ice before the isolation of monosomes. Subsequently, the monosome fraction was collected by sucrose-density-gradient (10–55% (w/v)) ultracentrifugation at 35,000 r.p.m. for 3 h, followed by a hot phenol–SDS extraction[207] to isolate the ribosome-protected mRNA fragments. The mRNA fragments (15–45 bp) were isolated from a 15% TBE–urea polyacrylamide gel. The 3′ ends of the purified fragments were dephosphorylated and ligated to the modified oligo. The cDNA libraries generated by Superscript III were circularized using CircLigase as described above. The rRNA products were depleted by a respective biotinylated oligo mix for *E. coli* and *P. protegens* Pf-5. The circularized DNA (5 µl) was amplified using Phusion HF DNA polymerase with the o231 primer and indexing primers for 7–10 cycles. The amplified products (125–150 bp) were recovered from an 8% TBE–urea polyacrylamide gel. The purified products were analysed with a BioAnalyzer and sequenced using a sequencing primer (CGACAGGTTCAGAGTTCTACAGTCCGACGATC) and an Illumina HiSeq 2500 in rapid-run mode. The sequences were aligned to reference sequences using Bowtie 1.1.2 with the parameters –k1 –m2 –v1. A centre-weighting approach was used to map the aligned footprint reads ranging from 22 to 42 nucleotides in length. To map the P-site of ribosomes from the footprint reads, 11 nucleotides from both ends were trimmed and the remaining nucleotides were given the same score, normalized to the length of the centre region. Aligned reads (10–45 nucleotides) were mapped to the reference with equal weighting for each nucleotide. A Python 3.4 script was used to perform the mapping. To generate the ribosome-profiling read profile for each *nif* cluster, the raw trace profiles were multiplied by 10^8 and normalized to the respective total reads from the coding sequences of each species. To calculate the ribosome density of each gene, read densities were first normalized in the following ways: (1) the first and last five codons of the gene were excluded for the calculation to remove the effects of translation initiation and termination, (2) a genome-wide read-density profile was fitted to an exponential function and the density at each nucleotide on a given gene was corrected using this function, and (3) if the average read density on a gene was higher than one, a 90% winsorization was applied to reduce the effect of outliers. The sum of the normalized reads on a gene was normalized to the gene length and the total read densities on the coding sequences to yield the ribosome density.

Calculation of genetic-part strengths based on sequencing data. The activity of a promoter is defined as the change in RNAP flux δJ around a transcription start site x_{tss}[208]. The promoter strength was calculated using:

$$\delta J = \frac{\gamma}{n}\left[\sum_{i=x_{tss}+1}^{x_{tss}+1+n} m(i) - \sum_{i=x_{tss}-1}^{x_0-1-n} m(i)\right] \quad (1)$$

where $m(i)$ is the number of transcripts at each position i from the FPKM-normalized transcriptomic profiles, $\gamma = 0.0067\ s^{-1}$ is the degradation rate of mRNA and n is the window length before and after x_{tss}. The window length was set to ten. The T_s is defined as the fold-decrease in transcription before and after a terminator, which can be quantified from the FPKM-normalized transcriptomic profiles as:

$$T_s = \frac{\sum_{i=x_1+1}^{x_1+n} m(i)}{\sum_{i=x_0-n}^{x_0-1} m(i)} \quad (2)$$

where x_0 and x_1 are the beginning and end positions of the terminator part, respectively. The translation efficiency was calculated by dividing the ribosome density by the FPKM.

Analysis of *nifH* expression. Complementation of NifA was tested using plasmid pMR131–133, which contains *sfgfp* fused to the *nifH* promoter in the *A. caulinodans* Δ*nifA* mutant. The inducible NifA/RpoN expression was provided by the plasmid pMR127, into which *sfgfp* driven by the *nifH* promoter was added to analyse *nifH* promoter activity, thereby yielding pMR134 (Supplementary Fig. 18). The IPTG-inducible system in the plasmids pMR127 and pMR134 was substituted with other inducible systems—including the salicylic acid-inducible, and nopaline- and octopine-inducible systems, yielding pMR128–130 and pMR135–137, respectively (Fig. 6c,d and Supplementary Fig. 18). Each of the plasmids were mobilized into *A. caulinodans* Δ*nifA*, which were cultured following the same protocol as that for the nitrogenase activity assays (described earlier). Following an overnight incubation in minimal medium with a nitrogen source, the cultures were diluted to an OD_{600} of 0.4 in 2 ml UMS medium plus 30 mM lactate, antibiotics and an inducer (for the inducible systems) in 10-ml glass vials with PTFE-silicone septa screw caps. The headspace in the vials was replaced with 99% argon plus 1% oxygen using a vacuum manifold. The vials were incubated with shaking at 250 r.p.m. for 9 h at 30 °C, after which 10-µl volumes of the culture were diluted in 150 µl PBS with 2 mg ml^{-1} kanamycin for analysis by flow cytometry. To test the activation of the *nifH* promoters by diverse NifA proteins, each of the plasmids pMR52, pMR54 and pMR89–91 were introduced into *E. coli* MG1655, and each of the plasmids pMR92–98 were introduced into *P. protegens* Pf-5 (Supplementary Fig. 15). The plasmid pMR104 was used to provide IPTG-inducible *nifA* expression in *E. coli*. The controller encoding the IPTG-inducible *nifA* was inserted into the genome of *P. protegens* Pf-5 using the plasmids pMR99–101 with the Tn7 system (described earlier). The inducibility of *nifH* expression was assessed by the reporter plasmids pMR108–110 and pMR105–107 for *E. coli* and *P. protegens* Pf-5, respectively (Supplementary Fig. 17). The IPTG-inducible system of the *nifA* controller plasmid pMR99 was replaced with the arabinose- and naringenin-inducible systems, yielding pMR102 and pMR103, respectively. These controllers were introduced into *P. protegens* Pf-5, and the reporter plasmid pMR107 was used to test the inducibility of the *nifH* promoter (Fig. 6c). Following overnight incubation in minimal medium with a nitrogen source, the cultures were diluted to an OD_{600} of 0.4 in 2 ml BB medium, antibiotics and an inducer (for the inducible systems) in 10-ml glass vials with PTFE-silicone septa screw caps. The headspace in the vials was replaced with either 100% argon (for *E. coli*) or 99% argon plus 1% oxygen (for *P. protegens* Pf-5) using a vacuum manifold. The vials were incubated with shaking at 250 r.p.m. for 9 h at 30 °C, after which 10-µl volumes of the cultures were diluted in 150 µl PBS with 2 mg ml^{-1} kanamycin for analysis by flow cytometry.

Sequence alignment. NifA sequences of *R. sphaeroides* 2.4.1 (RSP_0547) and *A. caulinodans* ORS571 (AZC_1049) were obtained from the NCBI. The NifA protein sequences were aligned using MUSCLE (https://www.ebi.ac.uk/Tools/msa/muscle/)[204] with default settings (Supplementary Fig. 13).

Reporting Summary. Further information on research design is available in the Nature Research Reporting Summary linked to this article.

Data availability

Additional data supporting this study are available from the corresponding author on reasonable request. The RNA-seq and ribosome-profiling data are available in the Sequence Read Archive with the accession code PRJNA579767: *K. oxytoca* native *nif* cluster, RNA-seq (SRX7032059, SRX7032060 and SRX7032061) and ribosome-profiling (SRX7034729, SRX7034730, SRX7034731 and SRX7034732); *K. oxytoca* refactored *nif* cluster v2.1, RNA-seq (SRX7036110) and ribosome-

profiling (SRX7036099); *K. oxytoca* refactored *nif* cluster v3.2, RNA-seq (SRX7035703, SRX7035704 and SRX7035705) and ribosome-profiling (SRX7036113, SRX7036114 and SRX7036115).

Received: 15 March 2019; Accepted: 4 November 2019;
Published online: 16 December 2019

References

1. Harlan, J. R. *Crops and Man* 2nd edn (American Society of Agronomy, 1992).
2. Simmonds, J. *Community Matters: a History of Biological Nitrogen Fixation and Nodulation Research, 1965 to 1995.* PhD thesis, Rensselaer Polytechnic Institute (2007).
3. Erisman, J., Bleeker, A., Galloway, J. & Sutton, M. Reduced nitrogen in ecology and the environment. *Environ. Pollut.* **150**, 140–149 (2007).
4. Geddes, B. A. et al. Use of plant colonizing bacteria as chassis for transfer of N_2-fixation to cereals. *Curr. Opin. Biotechnol.* **32**, 216–222 (2015).
5. Zaim, S., Bekkar, A. A. & Belabid, L. in *Rhizobium Biology and Biotechnology* (eds Hansen, A. P. et al.) 25–37 (Springer, 2017).
6. Nadarajah, K. K. in *Rhizobium Biology and Biotechnology* (eds Hansen, A. P. et al.) 83–103 (Springer, 2017).
7. Gutierrez-Zamora, M. & Martınez-Romero, E. Natural endophytic association between *Rhizobium etli* and maize (*Zea mays* L.). *J. Biotechnol.* **91**, 117–126 (2001).
8. McInroy, J. A. & Kloepper, J. W. Survey of indigenous bacterial endophytes from cotton and sweet corn. *Plant Soil* **173**, 337–342 (1995).
9. Ramachandran, V. K., East, A. K., Karunakaran, R., Downie, J. A. & Poole, P. S. Adaptation of *Rhizobium leguminosarum* to pea, alfalfa and sugar beet rhizospheres investigated by comparative transcriptomics. *Genome Biol.* **12**, R106 (2011).
10. Frans, J. et al. in *Nitrogen Fixation* (Ed. Gresshoff, P. M.) 33–44 (Springer, 1990).
11. Delmotte, N. et al. An integrated proteomics and transcriptomics reference data set provides new insights into the *Bradyrhizobium japonicum* bacteroid metabolism in soybean root nodules. *Proteomics* **10**, 1391–1400 (2010).
12. James, E. Nitrogen fixation in endophytic and associative symbiosis. *Field Crops Res.* **65**, 197–209 (2000).
13. Arsène, F., Katupitiya, S., Kennedy, I. R. & Elmerich, C. Use of *IacZ* fusions to study the expression of *nif* genes of *Azospirillum brasilense*. *Mol. Plant Microbe Interact.* **7**, 748–757 (1994).
14. Boddey, R. M. et al. in *Management of Biological Nitrogen Fixation for the Development of More Productive and Sustainable Agricultural Systems* (eds Ladha, J. K. & Peoples, M. B.) 195–209 (Springer, 1995).
15. Bremer, E., Janzen, H. & Gilbertson, C. Evidence against associative N_2 fixation as a significant N source in long-term wheat plots. *Plant Soil* **175**, 13–19 (1995).
16. Chalk, P. The contribution of associative and symbiotic nitrogen fixation to the nitrogen nutrition of non-legumes. *Plant Soil* **132**, 29–39 (1991).
17. Hurek, T., Reinhold-Hurek, B., Van Montagu, M. & Kellenberger, E. Root colonization and systemic spreading of *Azoarcus* sp. strain BH72 in grasses. *J. Bacteriol.* **176**, 1913–1923 (1994).
18. ames, E., Olivares, F., Baldani, J. & Döbereiner, J. *Herbaspirillum*, an endophytic diazotroph colonizing vascular tissue 3 *Sorghum bicolor* L. Moench. *J. Exp. Bot.* **48**, 785–798 (1997).
19. Kapulnik, Y., Feldman, M., Okon, Y. & Henis, Y. Contribution of nitrogen fixed by *Azospirillum* to the N nutrition of spring wheat in Israel. *Soil Biology Biochem.* **17**, 509–515 (1985).
20. Katupitiya, S. et al. A mutant of *Azospirillum brasilense* Sp7 impaired in flocculation with a modified colonization pattern and superior nitrogen fixation in association with wheat. *Appl. Environ. Microbiol.* **61**, 1987–1995 (1995).
21. Malik, K. et al. Association of nitrogen-fixing, plant-growth-promoting rhizobacteria (PGPR) with kallar grass and rice. *Plant Soil* **194**, 37–44 (1997).
22. Reinhold-Hurek, B. & Hurek, T. Interactions of gramineous plants with *Azoarcus* spp. and other diazotrophs: identification, localization, and perspectives to study their function. *Crit. Rev. Plant Sci.* **17**, 29–54 (1998).
23. Stoltzfus, J., So, R., Malarvithi, P., Ladha, J. & De Bruijn, F. Isolation of endophytic bacteria from rice and assessment of their potential for supplying rice with biologically fixed nitrogen. *Plant Soil* **194**, 25–36 (1997).
24. Triplett, E. W. Diazotrophic endophytes: progress and prospects for nitrogen fixation in monocots. *Plant Soil* **186**, 29–38 (1996).
25. Broek, A. V., Michiels, J., Van Gool, A. & Vanderleyden, J. Spatial-temporal colonization patterns of *Azospirillum brasilense* on the wheat root surface and expression of the bacterial *nifH* gene during association. *Mol. Plant Microbe Interact.* **6**, 592–600 (1993).
26. Yanni, Y. G. et al. in *Opportunities for Biological Nitrogen Fixation in Rice and Other Non-Legumes* (eds Ladha, J. K. et al.) 99–114 (Springer, 1997).
27. Okon, Y. *Azospirillum* as a potential inoculant for agriculture. *Trends Biotechnol.* **3**, 223–228 (1985).
28. Cocking, E. C. Endophytic colonization of plant roots by nitrogen-fixing bacteria. *Plant Soil* **252**, 169–175 (2003).
29. Woodard, H. & Bly, A. Maize growth and yield responses to seed-inoculated N_2-fixing bacteria under Dryland production conditions. *J. Plant Nutr.* **23**, 55–65 (2000).
30. Igiehon, N. O. & Babalola, O. O. Rhizosphere microbiome modulators: contributions of nitrogen fixing bacteria towards sustainable agriculture. *Int. J. Environ. Res. Public Health* **15**, 574 (2018).
31. Biswas, J., Ladha, J. & Dazzo, F. Rhizobia inoculation improves nutrient uptake and growth of lowland rice. *Soil Sci. Soc. Am. J.* **64**, 1644–1650 (2000).
32. Biswas, J. C., Ladha, J. K., Dazzo, F. B., Yanni, Y. G. & Rolfe, B. G. Rhizobial inoculation influences seedling vigor and yield of rice. *Agron. J.* **92**, 880–886 (2000).
33. Cummings, S. P. et al. Nodulation of *Sesbania* species by *Rhizobium* (*Agrobacterium*) strain IRBG74 and other rhizobia. *Environ. Microbiol.* **11**, 2510–2525 (2009).
34. Masson-Boivin, C., Giraud, E., Perret, X. & Batut, J. Establishing nitrogen-fixing symbiosis with legumes: how many rhizobium recipes? *Trends Microbiol.* **17**, 458–466 (2009).
35. Hoover, T. R., Imperial, J., Ludden, P. W. & Shah, V. K. Homocitrate is a component of the iron-molybdenum cofactor of nitrogenase. *Biochemistry* **28**, 2768–2771 (1989).
36. Mandon, K. et al. Role of the *fixGHI* region of *Azorhizobium caulinodans* in free-living and symbiotic nitrogen fixation. *FEMS Microbiol. Lett.* **114**, 185–189 (1993).
37. Tsukada, S. et al. Comparative genome-wide transcriptional profiling of *Azorhizobium caulinodans* ORS571 grown under free-living and symbiotic conditions. *Appl. Environ. Microbiol.* **75**, 5037–5046 (2009).
38. Gopalaswamy, G., Kannaiyan, S., O'Callaghan, K. J., Davey, M. R. & Cocking, E. C. The xylem of rice (*Oryza sativa*) is colonized by *Azorhizobium caulinodans*. *Proc. Biol. Sci.* **267**, 103–107 (2000).
39. Webster, G. et al. The flavonoid naringenin stimulates the intercellular colonization of wheat roots by *Azorhizobium caulinodans*. *Plant Cell Environ.* **21**, 373–383 (1998).
40. Webster, G. et al. in *Opportunities for Biological Nitrogen Fixation in Rice and Other Non-Legumes* (eds Ladha, J. K. et al.) 115–122 (Springer, 1997).
41. Triplett, E. W., Kaeppler, S. M. & Chelius, M. K. *Klebsiella pneumoniae* inoculants for enhancing plant growth. US patent 7,393,678 (2008).
42. Fujii, T. et al. Effect of inoculation with *Klebsiella oxytoca* and *Enterobacter cloacae* on dinitrogen fixation by rice–bacteria associations. *Plant Soil* **103**, 221–226 (1987).
43. El-Khawas, H. & Adachi, K. Identification and quantification of auxins in culture media of *Azospirillum* and *Klebsiella* and their effect on rice roots. *Biol. Fertil. Soils* **28**, 377–381 (1999).
44. Palus, J. A., Borneman, J., Ludden, P. W. & Triplett, E. W. A diazotrophic bacterial endophyte isolated from stems of *Zea mays* L. and *Zea luxurians* Iltis and Doebley. *Plant Soil* **186**, 135–142 (1996).
45. Rediers, H. et al. Development and application of a *dapB*-based in vivo expression technology system to study colonization of rice by the endophytic nitrogen-fixing bacterium *Pseudomonas stutzeri* A15. *Appl. Environ. Microbiol.* **69**, 6864–6874 (2003).
46. Haahtela, K. & Korhonen, T. K. In vitro adhesion of N_2-fixing enteric bacteria to roots of grasses and cereals. *Appl. Environ. Microbiol.* **49**, 1186–1190 (1985).
47. Desnoues, N. et al. Nitrogen fixation genetics and regulation in a *Pseudomonas stutzeri* strain associated with rice. *Microbiology* **149**, 2251–2262 (2003).
48. Paulsen, I. T. et al. Complete genome sequence of the plant commensal *Pseudomonas fluorescens* Pf-5. *Nat. Biotechnol.* **23**, 873 (2005).
49. Walsh, U. F., Morrissey, J. P. & O'Gara, F. *Pseudomonas* for biocontrol of phytopathogens: from functional genomics to commercial exploitation. *Curr. Opin. Biotechnol.* **12**, 289–295 (2001).
50. Dos Santos, P. C., Fang, Z., Mason, S. W., Setubal, J. C. & Dixon, R. Distribution of nitrogen fixation and nitrogenase-like sequences amongst microbial genomes. *BMC Genomics* **13**, 162 (2012).
51. Boyd, E. S., Costas, A. M. G., Hamilton, T. L., Mus, F. & Peters, J. W. Evolution of molybdenum nitrogenase during the transition from anaerobic to aerobic metabolism. *J. Bacteriol.* **197**, 1690–1699 (2015).
52. Raymond, J., Siefert, J. L., Staples, C. R. & Blankenship, R. E. The natural history of nitrogen fixation. *Molec. Biol. Evol.* **21**, 541–554 (2004).
53. Rubio, L. M. & Ludden, P. W. Biosynthesis of the iron-molybdenum cofactor of nitrogenase. *Annu. Rev. Microbiol.* **62**, 93–111 (2008).
54. Iki, T., Aono, T. & Oyaizu, H. Evidence for functional differentiation of duplicated *nifH* genes in *Azorhizobium caulinodans*. *FEMS Microbiol. Lett.* **274**, 173–179 (2007).
55. Ratet, P., Pawlowski, K., Schell, J. & Bruijn, F. The *Azorhizobium caulinodans* nitrogen-fixation regulatory gene, *nifA*, is controlled by the cellular nitrogen and oxygen status. *Mol. Microbiol.* **3**, 825–838 (1989).

56. Poudel, S. et al. Electron transfer to nitrogenase in different genomic and metabolic backgrounds. *J. Bacteriol.* **200**, 00757–00717 (2018).
57. Boyd, E. & Peters, J. W. New insights into the evolutionary history of biological nitrogen fixation. *Front. Microbiol.* **4**, 201 (2013).
58. Shah, V. K., Stacey, G. & Brill, W. J. Electron transport to nitrogenase. Purification and characterization of pyruvate: flavodoxin oxidoreductase. The *nifJ* gene product. *J. Biol. Chem.* **258**, 12064–12068 (1983).
59. Schmehl, M. et al. Identification of a new class of nitrogen fixation genes in *Rhodobacter capsulatus*: a putative membrane complex involved in electron transport to nitrogenase. *Mol. Gen. Genet.* **241**, 602–615 (1993).
60. Edgren, T. & Nordlund, S. The *fixABCX* genes in *Rhodospirillum rubrum* encode a putative membrane complex participating in electron transfer to nitrogenase. *J. Bacteriol.* **186**, 2052–2060 (2004).
61. Pascuan, C., Fox, A. R., Soto, G. & Ayub, N. D. Exploring the ancestral mechanisms of regulation of horizontally acquired nitrogenases. *J. Mol. Evol.* **81**, 84–89 (2015).
62. Yan, Y. et al. Nitrogen fixation island and rhizosphere competence traits in the genome of root-associated *Pseudomonas stutzeri* A1501. *Proc. Natl Acad. Sci. USA* **105**, 7564–7569 (2008).
63. Kechris, K. J., Lin, J. C., Bickel, P. J. & Glazer, A. N. Quantitative exploration of the occurrence of lateral gene transfer by using nitrogen fixation genes as a case study. *Proc. Natl Acad. Sci. USA* **103**, 9584–9589 (2006).
64. Thöny, B., Anthamatten, D. & Hennecke, H. Dual control of the *Bradyrhizobium japonicum* symbiotic nitrogen fixation regulatory operon *fixR nifA*: analysis of cis-and trans-acting elements. *J. Bacteriol.* **171**, 4162–4169 (1989).
65. Li, X.-X., Liu, Q., Liu, X.-M., Shi, H.-W. & Chen, S.-F. Using synthetic biology to increase nitrogenase activity. *Microb. Cell Fact.* **15**, 43 (2016).
66. Han, Y. et al. Interspecies transfer and regulation of *Pseudomonas stutzeri* A1501 nitrogen fixation Island in *Escherichia coli*. *J. Microbiol. Biotechnol.* **25**, 1339–1348 (2015).
67. Dixon, R. A. & Postgate, J. R. Genetic transfer of nitrogen fixation from *Klebsiella pneumoniae* to *Escherichia coli*. *Nature* **237**, 102 (1972).
68. Cannon, F., Dixon, R., Postgate, J. & Primrose, S. Chromosomal integration of *Klebsiella* nitrogen fixation genes in *Escherichia coli*. *Microbiology* **80**, 227–239 (1974).
69. Cannon, F., Dixon, R., Postgate, J. & Primrose, S. Plasmids formed in nitrogen-fixing *Escherichia coli–Klebsiella pneumoniae* hybrids. *Microbiology* **80**, 241–251 (1974).
70. Wang, L. et al. A minimal nitrogen fixation gene cluster from *Paenibacillus* sp. WLY78 enables expression of active nitrogenase in *Escherichia coli*. *PLoS Genet.* **9**, e1003865 (2013).
71. Temme, K., Zhao, D. & Voigt, C. A. Refactoring the nitrogen fixation gene cluster from *Klebsiella oxytoca*. *Proc. Natl Acad. Sci. USA* **109**, 7085–7090 (2012).
72. Smanski, M. J. et al. Functional optimization of gene clusters by combinatorial design and assembly. *Nat. Biotechnol.* **32**, 1241 (2014).
73. Zhang, L., Liu, X., Li, X. & Chen, S. Expression of the N_2 fixation gene operon of *Paenibacillus* sp. WLY78 under the control of the T7 promoter in *Escherichia coli* BL21. *Biotechnol. Lett.* **37**, 1999–2004 (2015).
74. Postgate, J. R. & Kent, H. M. Qualitative evidence for expression of *Klebsiella pneumoniae nif* in *Pseudomonas putida*. *Microbiology* **133**, 2563–2566 (1987).
75. Setten, L. et al. Engineering *Pseudomonas protegens* Pf-5 for nitrogen fixation and its application to improve plant growth under nitrogen-deficient conditions. *PLoS ONE* **8**, e63666 (2013).
76. Dixon, R. & Kahn, D. Genetic regulation of biological nitrogen fixation. *Nat. Rev. Microbiol.* **2**, 621–631 (2004).
77. Fischer, H.-M. Environmental regulation of rhizobial symbiotic nitrogen fixation genes. *Trends Microbiol.* **4**, 317–320 (1996).
78. Tsoy, O. V., Ravcheev, D. A., Čuklina, J. & Gelfand, M. S. Nitrogen fixation and molecular oxygen: comparative genomic reconstruction of transcription regulation in Alphaproteobacteria. *Front. Microbiol.* **7**, 1343 (2016).
79. Hill, S., Kennedy, C., Kavanagh, E., Goldberg, R. B. & Hanau, R. Nitrogen fixation gene (*nifL*) involved in oxygen regulation of nitrogenase synthesis in *K. peumoniae*. *Nature* **290**, 424–426 (1981).
80. Mandon, K. et al. Poly-β-hydroxybutyrate turnover in *Azorhizobium caulinodans* is required for growth and affects *nifA* expression. *J. Bacteriol.* **180**, 5070–5076 (1998).
81. Little, R., Reyes-Ramirez, F., Zhang, Y., van Heeswijk, W. C. & Dixon, R. Signal transduction to the *Azotobacter vinelandii* NIFL–NIFA regulatory system is influenced directly by interaction with 2-oxoglutarate and the PII regulatory protein. *EMBO J.* **19**, 6041–6050 (2000).
82. Poole, P., Ramachandran, V. & Terpolilli, J. Rhizobia: from saprophytes to endosymbionts. *Nat. Rev. Microbiol.* **16**, 291–303 (2018).
83. Kong, Q., Wu, Q., Ma, Z. & Shen, S. Oxygen sensitivity of the *nifLA* promoter of *Klebsiella pneumoniae*. *J. Bacteriol.* **166**, 353–356 (1986).
84. Brooks, S. J., Collins, J. J. & Brill, W. J. Repression of nitrogen fixation in *Klebsiella pneumoniae* at high temperature. *J. Bacteriol.* **157**, 460–464 (1984).
85. Peoples, M., Ladha, J. & Herridge, D. Biological nitrogen fixation: an efficient source of nitrogen for sustainable agricultural production? *Plant Soil* **174**, 3–28 (1995).
86. Barakat, M., Cheviron, B. & Angulo-Jaramillo, R. Influence of the irrigation technique and strategies on the nitrogen cycle and budget: a review. *Agric. Water Manag.* **178**, 225–238 (2016).
87. Burger, M. & Jackson, L. E. Microbial immobilization of ammonium and nitrate in relation to ammonification and nitrification rates in organic and conventional cropping systems. *Soil Biol. Biochem.* **35**, 29–36 (2003).
88. MacNeil, D. & Brill, W. Mutations in *nif* genes that cause *Klebsiella pneumoniae* to be derepressed for nitrogenase synthesis in the presence of ammonium. *J. Bacteriol.* **144**, 744–751 (1980).
89. Bali, A., Blanco, G., Hill, S. & Kennedy, C. Excretion of ammonium by a *nifL* mutant of *Azotobacter vinelandii* fixing nitrogen. *Appl. Environ. Microbiol.* **58**, 1711–1718 (1992).
90. Brewin, B., Woodley, P. & Drummond, M. The basis of ammonium release in *nifL* mutants of *Azotobacter vinelandii*. *J. Bacteriol.* **181**, 7356–7362 (1999).
91. Arsène, F., Kaminski, P. A. & Elmerich, C. Control of *Azospirillum brasilense* NifA activity by PII: effect of replacing Tyr residues of the NifA N-terminal domain on NifA activity. *FEMS Microbiol. Lett.* **179**, 339–343 (1999).
92. Souza, E., Pedrosa, F., Drummond, M., Rigo, L. & Yates, M. Control of *Herbaspirillum seropedicae* NifA activity by ammonium ions and oxygen. *J. Bacteriol.* **181**, 681–684 (1999).
93. Paschen, A., Drepper, T., Masepohl, B. & Klipp, W. *Rhodobacter capsulatus nifA* mutants mediating *nif* gene expression in the presence of ammonium. *FEMS Microbiol. Lett.* **200**, 207–213 (2001).
94. Rey, F. E., Heiniger, E. K. & Harwood, C. S. Redirection of metabolism for biological hydrogen production. *Appl. Environ. Microbiol.* **73**, 1665–1671 (2007).
95. Smanski, M. J. et al. Synthetic biology to access and expand nature's chemical diversity. *Nat. Rev. Microbiol.* **14**, 135–149 (2016).
96. Scupham, A. J. et al. Inoculation with *Sinorhizobium meliloti* RMBPC-2 increases alfalfa yield compared with inoculation with a nonengineered wild-type strain. *Appl. Environ. Microbiol.* **62**, 4260–4262 (1996).
97. Fox, A. R. et al. Major cereal crops benefit from biological nitrogen fixation when inoculated with the nitrogen-fixing bacterium *Pseudomonas protegens* Pf-5 X940. *Environ. Microbiol.* **18**, 3522–3534 (2016).
98. Suthar, H., Hingurao, K., Vaghashiya, J. & Parmar, J. Fermentation: a process for biofertilizer production. *Microorg. Green Revol.* **6**, 229–252 (2017).
99. Lucy, M., Reed, E. & Glick, B. R. Applications of free living plant growth-promoting rhizobacteria. *Antonie Van Leeuwenhoek* **86**, 1–25 (2004).
100. Mahmood, A., Turgay, O. C., Farooq, M. & Hayat, R. Seed biopriming with plant growth promoting rhizobacteria: a review. *FEMS Microbiol. Ecol.* **92**, fiw112 (2016).
101. Velusamy, P., Immanuel, J. E., Gnanamanickam, S. S. & Thomashow, L. Biological control of rice bacterial blight by plant-associated bacteria producing 2, 4-diacetylphloroglucinol. *Can. J. Microbiol.* **52**, 56–65 (2006).
102. Mishra, J. *Development and Evaluation of Pseudomonas Based Bioformulation for Disease Control and Growth Enhancement of Zea Mays L.* PhD thesis, Babasaheb Bhimrao Ambedkar University (2016).
103. Weller, D. M. et al. Role of 2,4-diacetylphloroglucinol-producing fluorescent *Pseudomonas* spp. in the defense of plant roots. *Plant Biol.* **9**, 4–20 (2007).
104. Kaiser, C. et al. Exploring the transfer of recent plant photosynthates to soil microbes: mycorrhizal pathway vs direct root exudation. *New Phytol.* **205**, 1537–1551 (2015).
105. Mus, F. et al. Symbiotic nitrogen fixation and the challenges to its extension to nonlegumes. *Appl. Environ. Microbiol.* **82**, 3698–3710 (2016).
106. Perrine-Walker, F. M., Prayitno, J., Rolfe, B. G., Weinman, J. J. & Hocart, C. H. Infection process and the interaction of rice roots with rhizobia. *J. Exp. Bot.* **58**, 3343–3350 (2007).
107. Gough, C. et al. Specific flavonoids promote intercellular root colonization of *Arabidopsis thaliana* by *Azorhizobium caulinodans* ORS571. *Mol. Plant Microbe Interact.* **10**, 560–570 (1997).
108. O'Callaghan, K. J. et al. Effects of glucosinolates and flavonoids on colonization of the roots of *Brassica napus* by *Azorhizobium caulinodans* ORS571. *Appl. Environ. Microbiol.* **66**, 2185–2191 (2000).
109. Mongiardini, E. J. et al. The rhizobial adhesion protein RapA1 is involved in adsorption of rhizobia to plant roots but not in nodulation. *FEMS Microbiol. Ecol.* **65**, 279–288 (2008).
110. Matilla, M. A., Espinosa-Urgel, M., Rodríguez-Herva, J. J., Ramos, J. L. & Ramos-González, M. I. Genomic analysis reveals the major driving forces of bacterial life in the rhizosphere. *Genome Biol.* **8**, R179 (2007).
111. Casas, M. I., Duarte, S., Doseff, A. I. & Grotewold, E. Flavone-rich maize: an opportunity to improve the nutritional value of an important commodity crop. *Front. Plant Sci.* **5**, 440 (2014).
112. Ogo, Y., Ozawa, K., Ishimaru, T., Murayama, T. & Takaiwa, F. Transgenic rice seed synthesizing diverse flavonoids at high levels: a new platform for

flavonoid production with associated health benefits. *Plant Biotechnol. J.* **11**, 734–746 (2013).
113. Bacilio-Jiménez, M. et al. Chemical characterization of root exudates from rice (*Oryza sativa*) and their effects on the chemotactic response of endophytic bacteria. *Plant Soil* **249**, 271–277 (2003).
114. Pini, F. et al. Lux bacterial biosensors for in vivo spatiotemporal mapping of root secretion. *Plant Physiol.* **174**, 1289–1306 (2017).
115. Ryan, P. R., Dessaux, Y., Thomashow, L. S. & Weller, D. M. Rhizosphere engineering and management for sustainable agriculture. *Plant Soil* **321**, 363–383 (2009).
116. Dessaux, Y., Grandclément, C. & Faure, D. Engineering the rhizosphere. *Trends Plant Sci.* **21**, 266–278 (2016).
117. Geddes, B. A. et al. Engineering transkingdom signalling in plants to control gene expression in rhizosphere bacteria. *Nat. Comm.* **10**, 3430 (2019).
118. Arnold, W., Rump, A., Klipp, W., Priefer, U. B. & Pühler, A. Nucleotide sequence of a 24,206-base-pair DNA fragment carrying the entire nitrogen fixation gene cluster of *Klebsiella pneumoniae*. *J. Mol. Biol.* **203**, 715–738 (1988).
119. de Salamone, I. G., Döbereiner, J., Urquiaga, S. & Boddey, R. M. Biological nitrogen fixation in *Azospirillum* strain-maize genotype associations as evaluated by the ^{15}N isotope dilution technique. *Biol. Fert. Soils* **23**, 249–256 (1996).
120. Pedrosa, F. & Elmerich, C. in *Associative and Endophytic Nitrogen-fixing Bacteria and Cyanobacterial Associations* (eds Elmerich, C. & Newton, W. E.) 41–71 (Springer, 2007).
121. Welsh, E. A. et al. The genome of *Cyanothece* 51142, a unicellular diazotrophic cyanobacterium important in the marine nitrogen cycle. *Proc. Natl Acad. Sci. USA* **105**, 15094–15099 (2008).
122. Hamilton, T. L. et al. Transcriptional profiling of nitrogen fixation in *Azotobacter vinelandii*. *J. Bacteriol.* **193**, 4477–4486 (2011).
123. Oda, Y. et al. Functional genomic analysis of three nitrogenase isozymes in the photosynthetic bacterium *Rhodopseudomonas palustris*. *J. Bacteriol.* **187**, 7784–7794 (2005).
124. Haselkorn, R. & Kapatral, V. in *Genomes and Genomics of Nitrogen-fixing Organisms* (eds Palacios, R. & Newton, W. E.) 71–82 (Springer, 2005).
125. Jeong, H.-S. & Jouanneau, Y. Enhanced nitrogenase activity in strains of *Rhodobacter capsulatus* that overexpress the *rnf* genes. *J. Bacteriol.* **182**, 1208–1214 (2000).
126. Curatti, L., Brown, C. S., Ludden, P. W. & Rubio, L. M. Genes required for rapid expression of nitrogenase activity in *Azotobacter vinelandii*. *Proc. Natl Acad. Sci. USA* **102**, 6291–6296 (2005).
127. Kaminski, P. A. et al. Characterization of the *fixABC* region of *Azorhizobium caulinodans* ORS571 and identification of a new nitrogen fixation gene. *Mol. Gen. Genet.* **214**, 496–502 (1988).
128. Wientjens, R. *The Involvement of the fixABCX Genes and the Respiratory Chain in the Electron Transport to Nitrogenase in Azotobacter vinelandii*. PhD thesis, Agricultural University (1993).
129. McDermott, J. E. et al. A model of cyclic transcriptomic behavior in the cyanobacterium *Cyanothece* sp. ATCC 51142. *Mol. Biosyst.* **7**, 2407–2418 (2011).
130. Sevilla, M., Burris, R. H., Gunapala, N. & Kennedy, C. Comparison of benefit to sugarcane plant growth and $^{15}N_2$ incorporation following inoculation of sterile plants with *Acetobacter diazotrophicus* wild-type and *nif* mutant strains. *Mol. Plant Microbe Interact.* **14**, 358–366 (2001).
131. Eskin, N., Vessey, K. & Tian, L. Research progress and perspectives of nitrogen fixing bacterium, *Gluconacetobacter diazotrophicus*, in monocot plants. *Int. J. Agron.* https://doi.org/10.1155/2014/208383 (2014).
132. Lee, S., Reth, A., Meletzus, D., Sevilla, M. & Kennedy, C. Characterization of a major cluster of *nif, fix*, and associated genes in a sugarcane endophyte, *Acetobacter diazotrophicus*. *J. Bacteriol.* **182**, 7088–7091 (2000).
133. Shanks, R. M. et al. *Saccharomyces cerevisiae*-based molecular tool kit for manipulation of genes from gram-negative bacteria. *Appl. Environ. Microbiol.* **72**, 5027–5036 (2006).
134. Hakoyama, T. et al. Host plant genome overcomes the lack of a bacterial gene for symbiotic nitrogen fixation. *Nature* **462**, 514–517 (2009).
135. Li, G.-W., Oh, E. & Weissman, J. S. The anti-Shine–Dalgarno sequence drives translational pausing and codon choice in bacteria. *Nature* **484**, 538–541 (2012).
136. Lalanne, J.-B. et al. Evolutionary convergence of pathway-specific enzyme expression stoichiometry. *Cell* **173**, 749–761 (2018).
137. Li, G.-W., Burkhardt, D., Gross, C. & Weissman, J. S. Quantifying absolute protein synthesis rates reveals principles underlying allocation of cellular resources. *Cell* **157**, 624–635 (2014).
138. Poza-Carrión, C., Jiménez-Vicente, E., Navarro-Rodríguez, M., Echavarri-Erasun, C. & Rubio, L. M. Kinetics of *nif* gene expression in a nitrogen-fixing bacterium. *J. Bacteriol.* **196**, 595–603 (2014).
139. Tezcan, F. A., Kaiser, J. T., Howard, J. B. & Rees, D. C. Structural evidence for asymmetrical nucleotide interactions in nitrogenase. *J. Am. Chem. Soc.* **137**, 146–149 (2014).
140. Klugkist, J. & Haaker, H. Inhibition of nitrogenase activity by ammonium chloride in *Azotobacter vinelandii*. *J. Bacteriol.* **157**, 148–151 (1984).
141. Song, M. et al. Control of type III protein secretion using a minimal genetic system. *Nat. Comm.* **8**, 14737 (2017).
142. Guo, C.-J. et al. Discovery of reactive microbiota-derived metabolites that inhibit host proteases. *Cell* **168**, 517–526 (2017).
143. Ren, H., Hu, P. & Zhao, H. A plug-and-play pathway refactoring workflow for natural product research in *Escherichia coli* and *Saccharomyces cerevisiae*. *Biotechnol. Bioeng.* **114**, 1847–1854 (2017).
144. MacLellan, S. R., MacLean, A. M. & Finan, T. M. Promoter prediction in the rhizobia. *Microbiology* **152**, 1751–1763 (2006).
145. Ramírez-Romero, M. A., Masulis, I., Cevallos, M. A., González, V. & Davila, G. The *Rhizobium etli* σ70 (SigA) factor recognizes a lax consensus promoter. *Nucleic Acids Res.* **34**, 1470–1480 (2006).
146. Becker, A. et al. Riboregulation in plant-associated α-proteobacteria. *RNA Biol.* **11**, 550–562 (2014).
147. Robledo, M., Frage, B., Wright, P. R. & Becker, A. A stress-induced small RNA modulates alpha-rhizobial cell cycle progression. *PLoS Genet.* **11**, e1005153 (2015).
148. Giacomini, A., Ollero, F. J., Squartini, A. & Nuti, M. P. Construction of multipurpose gene cartridges based on a novel synthetic promoter for high-level gene expression in Gram-negative bacteria. *Gene* **144**, 17–24 (1994).
149. Khan, S. R., Gaines, J., Roop, R. M. & Farrand, S. K. Broad-host-range expression vectors with tightly regulated promoters and their use to examine the influence of TraR and TraM expression on Ti plasmid quorum sensing. *Appl. Environ. Microbiol.* **74**, 5053–5062 (2008).
150. Tett, A. J. et al. Regulatable vectors for environmental gene expression in Alphaproteobacteria. *Appl. Environ. Microbiol.* **78**, 7137–7140 (2012).
151. Mostafavi, M. et al. Analysis of a taurine-dependent promoter in *Sinorhizobium meliloti* that offers tight modulation of gene expression. *BMC Microbiol.* **14**, 295 (2014).
152. Anderson, J. et al. BglBricks: a flexible standard for biological part assembly. *J. Biol. Eng.* **4**, 1 (2010).
153. Farasat, I. et al. Efficient search, mapping, and optimization of multi-protein genetic systems in diverse bacteria. *Mol. Sys. Biol.* **10**, 731 (2014).
154. Cambray, G. et al. Measurement and modeling of intrinsic transcription terminators. *Nucleic Acids Res.* **41**, 5139–5148 (2013).
155. Chen, Y.-J. et al. Characterization of 582 natural and synthetic terminators and quantification of their design constraints. *Nat. Methods* **10**, 659–664 (2013).
156. Temme, K., Hill, R., Segall-Shapiro, T. H., Moser, F. & Voigt, C. A. Modular control of multiple pathways using engineered orthogonal T7 polymerases. *Nucleic Acids Res.* **40**, 8773–8781 (2012).
157. Price, M. N., Arkin, A. P. & Alm, E. The life-cycle of operons. *PLoS Genet.* **2**, e96 (2006).
158. Touchon, M. & Rocha, E. P. Coevolution of the organization and structure of prokaryotic genomes. *Cold Spring Harb. Persp. Biol.* **8**, a018168 (2016).
159. Price, M. N., Huang, K. H., Arkin, A. P. & Alm, E. Operon formation is driven by co-regulation and not by horizontal gene transfer. *Genome Res.* **15**, 809–819 (2005).
160. Kaminski, P. A. & Elmerich, C. The control of *Azorhizobium caulinodans nifA* expression by oxygen, ammonia and by the HF-I-like protein, NrfA. *Mol. Microbiol.* **28**, 603–613 (1998).
161. Pawlowski, K., Klosse, U. & De Bruijn, F. J. Characterization of a novel *Azorhizobium caulinodans* ORS571 two-component regulatory system, NtrY/NtrX, involved in nitrogen fixation and metabolism. *Mol. Gen. Genet.* **231**, 124–138 (1991).
162. Kaminski, P. & Elmerich, C. Involvement of *fixLJ* in the regulation of nitrogen fixation in *Azorhizobium caulinodans*. *Mol. Microbiol.* **5**, 665–673 (1991).
163. Kaminski, P., Mandon, K., Arigoni, F., Desnoues, N. & Elmerich, C. Regulation of nitrogen fixation in *Azorhizobium caulinodans*: identification of a *fixK*-like gene, a positive regulator of nifA. *Mol. Microbiol.* **5**, 1983–1991 (1991).
164. Michel-Reydellet, N. & Kaminski, P. A. J. *Azorhizobium caulinodans* PII and GlnK proteins control nitrogen fixation and ammonia assimilation. *J. Bacteriol.* **181**, 2655–2658 (1999).
165. Drepper, T. et al. Role of GlnB and GlnK in ammonium control of both nitrogenase systems in the phototrophic bacterium *Rhodobacter capsulatus*. *Microbiology* **149**, 2203–2212 (2003).
166. Martínez-García, E. & de Lorenzo, V. Molecular tools and emerging strategies for deep genetic/genomic refactoring of *Pseudomonas*. *Curr. Opin. Biotechnol.* **47**, 120–132 (2017).
167. Calero, P., Jensen, S. I. & Nielsen, A. T. Broad-host-range ProUSER vectors enable fast characterization of inducible promoters and optimization of p-coumaric acid production in *Pseudomonas putida* KT2440. *ACS Synth. Biol.* **5**, 741–753 (2016).
168. Choi, K.-H. & Schweizer, H. P. mini-Tn7 insertion in bacteria with single attTn7 sites: example *Pseudomonas aeruginosa*. *Nat. Protoc.* **1**, 153–161 (2006).

169. Poole, R. K. & Hill, S. Respiratory protection of nitrogenase activity in *Azotobacter vinelandii*—roles of the terminal oxidases. *Biosci. Rep.* **17**, 303–317 (1997).
170. Sabra, W., Zeng, A.-P., Lünsdorf, H. & Deckwer, W.-D. Effect of oxygen on formation and structure of *Azotobacter vinelandii* alginate and its role in protecting nitrogenase. *Appl. Environ. Microbiol.* **66**, 4037–4044 (2000).
171. Schlesier, J., Rohde, M., Gerhardt, S. & Einsle, O. A conformational switch triggers nitrogenase protection from oxygen damage by Shethna protein II (FeSII). *J. Am. Chem. Soc.* **138**, 239–247 (2015).
172. Ledbetter, R. N. et al. The electron bifurcating FixABCX protein complex from *Azotobacter vinelandii*: generation of low-potential reducing equivalents for nitrogenase catalysis. *Biochemistry* **56**, 4177–4190 (2017).
173. Li, B. et al. Root exudates drive interspecific facilitation by enhancing nodulation and N_2 fixation. *Proc. Natl Acad. Sci. USA* **113**, 6496–6501 (2016).
174. Wang, Y., Zhang, J., Sun, Y., Feng, J. & Zhang, X. Evaluating the potential value of vatural product cuminic acid against plant pathogenic fungi in cucumber. *Molecules* **22**, 1914 (2017).
175. Zhou, X. & Wu, F. Vanillic acid changed cucumber (*Cucumis sativus* L.) seedling rhizosphere total bacterial, *Pseudomonas* and *Bacillus* spp. communities. *Sci. Rep.* **8**, 4929 (2018).
176. Sun, Y., Wang, Y., Han, L., Zhang, X. & Feng, J. Antifungal activity and action mode of cuminic acid from the seeds of *Cuminum cyminum* L. against *Fusarium oxysporum* f. sp. *Niveum* (FON) causing fusarium wilt on watermelon. *Molecules* **22**, 2053 (2017).
177. Wang, Y., Sun, Y., Zhang, Y., Zhang, X. & Feng, J. Antifungal activity and biochemical response of cuminic acid against *Phytophthora capsici* Leonian. *Molecules* **21**, 756 (2016).
178. Bais, H. P., Weir, T. L., Perry, L. G., Gilroy, S. & Vivanco, J. M. The role of root exudates in rhizosphere interactions with plants and other organisms. *Annu. Rev. Plant Biol.* **57**, 233–266 (2006).
179. Rasmann, S. & Turlings, T. C. Root signals that mediate mutualistic interactions in the rhizosphere. *Curr. Opin. Plant Biol.* **32**, 62–68 (2016).
180. Soto, M. J., Sanjuan, J. & Olivares, J. Rhizobia and plant-pathogenic bacteria: common infection weapons. *Microbiology* **152**, 3167–3174 (2006).
181. Poonguzhali, S., Madhaiyan, M. & Sa, T. Quorum-sensing signals produced by plant-growth promoting *Burkholderia* strains under in vitro and in planta conditions. *Res. Microbiol.* **158**, 287–294 (2007).
182. Sanchez-Contreras, M., Bauer, W. D., Gao, M., Robinson, J. B. & Allan Downie, J. Quorum-sensing regulation in rhizobia and its role in symbiotic interactions with legumes. *Philos. Trans. R. Soc. B* **362**, 1149–1163 (2007).
183. Chagas, F. O., de Cassia Pessotti, R., Caraballo-Rodríguez, A. M. & Pupo, M. T. Chemical signaling involved in plant–microbe interactions. *Chem. Soc. Rev.* **47**, 1652–1704 (2018).
184. Schikora, A., Schenk, S. T. & Hartmann, A. Beneficial effects of bacteria–plant communication based on quorum sensing molecules of the *N*-acyl homoserine lactone group. *Plant Mol. Biol.* **90**, 605–612 (2016).
185. Westervelt, P., Bloom, M. L., Mabbott, G. A. & Fekete, F. A. The isolation and identification of 3, 4-dihydroxybenzoic acid formed by nitrogen-fixing *Azomonas macrocytogenes*. *FEMS Microbiol. Lett.* **30**, 331–335 (1985).
186. Collinson, S. K., Doran, J. L. & Page, W. J. Production of 3, 4-dihydroxybenzoic acid by *Azomonas macrocytogenes* and *Azotobacter paspali*. *Can. J. Microbiol.* **33**, 169–175 (1987).
187. Bhattacharya, A., Sood, P. & Citovsky, V. The roles of plant phenolics in defence and communication during *Agrobacterium* and *Rhizobium* infection. *Mol. Plant Path.* **11**, 705–719 (2010).
188. Mathesius, U. et al. Extensive and specific responses of a eukaryote to bacterial quorum-sensing signals. *Proc. Natl Acad. Sci. USA* **100**, 1444–1449 (2003).
189. Hernández-Reyes, C., Schenk, S. T., Neumann, C., Kogel, K. H. & Schikora, A. *N*-acyl-homoserine lactones-producing bacteria protect plants against plant and human pathogens. *Microbial Biotechnol.* **7**, 580–588 (2014).
190. Pérez-Montaño, F. et al. Rice and bean AHL-mimic quorum-sensing signals specifically interfere with the capacity to form biofilms by plant-associated bacteria. *Res. Microbiol.* **164**, 749–760 (2013).
191. Bressan, M. et al. Exogenous glucosinolate produced by *Arabidopsis thaliana* has an impact on microbes in the rhizosphere and plant roots. *ISME J.* **3**, 1243–1257 (2009).
192. Badri, D. V. et al. An ABC transporter mutation alters root exudation of phytochemicals that provoke an overhaul of natural soil microbiota. *Plant Physiol.* **151**, 2006–2017 (2009).
193. Abdel-Ghany, S. E., Day, I., Heuberger, A. L., Broeckling, C. D. & Reddy, A. S. Production of phloroglucinol, a platform chemical, in *Arabidopsis* using a bacterial gene. *Sci. Rep.* **6**, 38483 (2016).
194. Oger, P., Petit, A. & Dessaux, Y. Genetically engineered plants producing opines alter their biological environment. *Nat. Biotechnol.* **15**, 369 (1997).
195. Mondy, S. et al. An increasing opine carbon bias in artificial exudation systems and genetically modified plant rhizospheres leads to an increasing reshaping of bacterial populations. *Mol. Ecol.* **23**, 4846–4861 (2014).
196. Meyer, A. J., Segall-Shapiro, T. H., Glassey, E., Zhang, J. & Voigt, C. A. *Escherichia coli* "Marionette" strains with 12 highly optimized small-molecule sensors. *Nat. Chem. Biol.* **15**, 196–204 (2018).
197. Poole, P. S., Schofiel, N. A., Reid, C. J., Drew, E. M. & Walshaw, D. L. Identification of chromosomal genes located downstream of *dctD* that affect the requirement for calcium and the lipopolysaccharide layer of *Rhizobium leguminosarum*. *Microbiology* **140**, 2797–2809 (1994).
198. Wilson, P. W. & Knight, S. G. *Experiments in Bacterial Physiology* (Burgess, 1952).
199. Udvardi, M. & Poole, P. S. Transport and metabolism in legume-rhizobia symbioses. *Ann. Rev. Plant Biol.* **64**, 781–805 (2013).
200. Ferri, L., Gori, A., Biondi, E. G., Mengoni, A. & Bazzicalupo, M. Plasmid electroporation of *Sinorhizobium* strains: the role of the restriction gene *hsdR* in type strain Rm1021. *Plasmid* **63**, 128–135 (2010).
201. Selbitschka, W. et al. Characterization of *recA* genes and *recA* mutants of *Rhizobium meliloti* and *Rhizobium leguminosarum* biovar viciae. *Mol. Gen. Genet.* **229**, 86–95 (1991).
202. Prell, J., Boesten, B., Poole, P. & Priefer, U. B. The *Rhizobium leguminosarum* bv. viciae VF39 γ-aminobutyrate (GABA) aminotransferase gene (*gabT*) is induced by GABA and highly expressed in bacteroids. *Microbiology* **148**, 615–623 (2002).
203. Silva-Rocha, R. et al. The Standard European Vector Architecture (SEVA): a coherent platform for the analysis and deployment of complex prokaryotic phenotypes. *Nucleic Acids Res.* **41**, D666–D675 (2012).
204. Edgar, R. C. MUSCLE: multiple sequence alignment with high accuracy and high throughput. *Nucleic Acids Res.* **32**, 1792–1797 (2004).
205. Yan, Y. et al. Global transcriptional analysis of nitrogen fixation and ammonium repression in root-associated *Pseudomonas stutzeri* A1501. *BMC Genomics* **11**, 11 (2010).
206. Jacob, G., Schaefer, J., Garbow, J. & Stejskal, E. Solid-state NMR studies of *Klebsiella pneumoniae* grown under nitrogen-fixing conditions. *J. Biol. Chem.* **262**, 254–259 (1987).
207. Blomberg, P., Wagner, E. & Nordström, K. Control of replication of plasmid R1: the duplex between the antisense RNA, CopA, and its target, CopT, is processed specifically in vivo and in vitro by RNase III. *EMBO J.* **9**, 2331–2340 (1990).
208. Gorochowski, T. E. et al. Genetic circuit characterization and debugging using RNA-seq. *Mol. Syst. Biol.* **13**, 952 (2017).

Acknowledgements

This work was supported by the National Science Foundation (grant no. NSF-1331098), the Abdul Latif Jameel Water and Food Security Lab (J-WAFS) at the Massachusetts Institute of Technology, the US National Science Foundation Synthetic Biology Engineering Research Center (grant no. SynBERC EEC0540879) and the Office of Naval Research Multidisciplinary University Research Initiative (MURI grant no. N00014-13-1-0074). We thank G. O'Toole of Dartmouth College for the yeast shuttle vectors.

Author contributions

M.-H.R. and C.A.V. conceived the study and designed the experiments. J.Z. and M.-H.R. performed the RNA-seq and ribosome-profiling experiments and analysed the data. T.T. and M.-H.R. performed the opine experiments and analysed the data. D.K., J.-M.A., F.M. and J.W.P. performed the ^{15}N-incorporation experiments and analysed the data. B.A.G. and P.S.P. performed the diazotrophic growth experiments and analysed the data. M.-H.R. performed all other experiments and analysed the data. M.-H.R. and C.A.V. wrote the manuscript with input from all of the authors.

Competing interests

M.-H.R. and C.A.V. have filed a patent application (US provisional application no. 62/820,765) on this work.

Additional information

Extended data is available for this paper at https://doi.org/10.1038/s41564-019-0631-2.

Supplementary information is available for this paper at https://doi.org/10.1038/s41564-019-0631-2.

Correspondence and requests for materials should be addressed to C.A.V.

Reprints and permissions information is available at www.nature.com/reprints.

Publisher's note Springer Nature remains neutral with regard to jurisdictional claims in published maps and institutional affiliations.

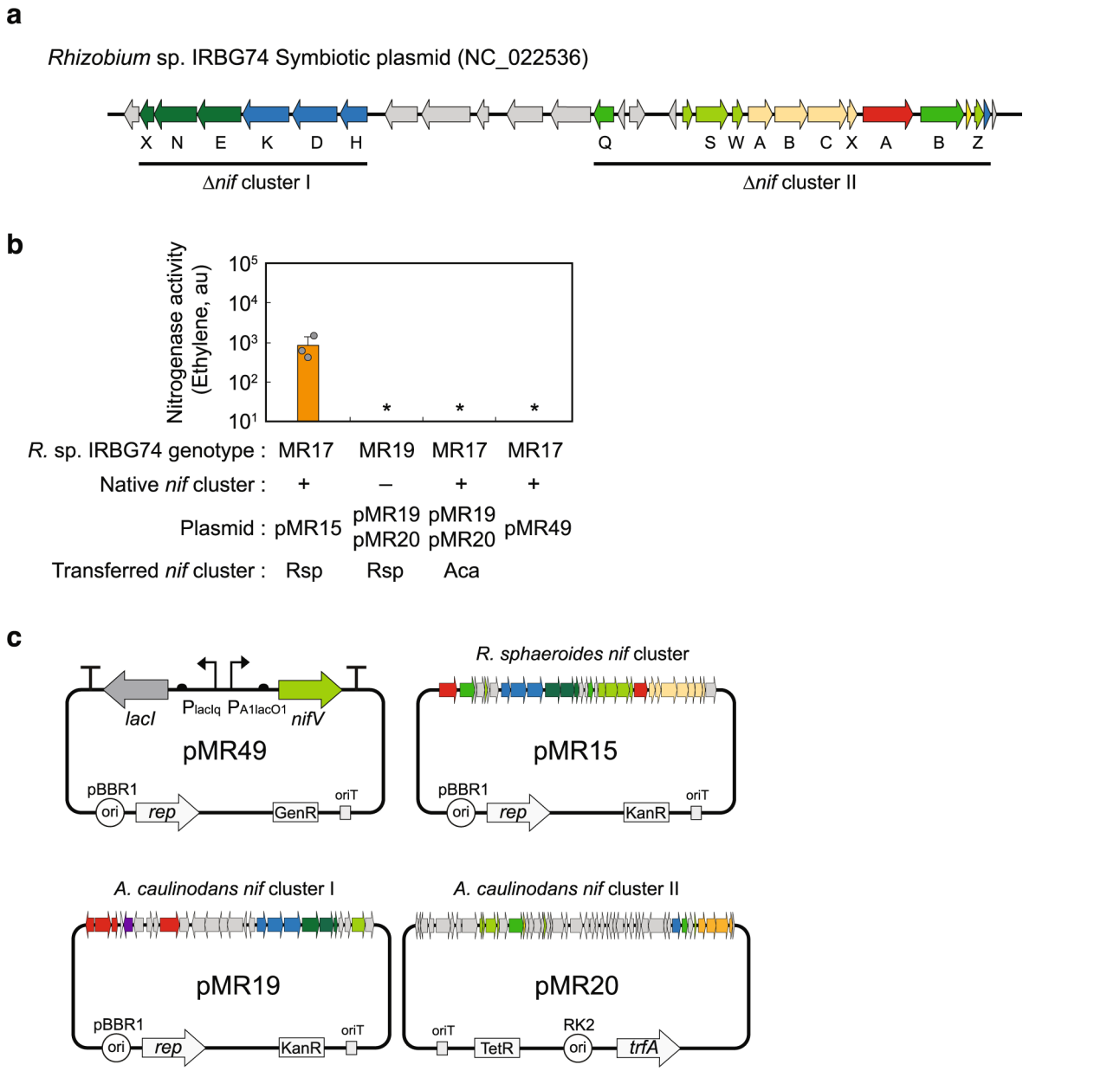

Extended Data Fig. 1 | Nitrogenase activity in wild-type *R.* sp. IRBG74 and a Δ*nif* mutant strain, in which the native *nif* clusters are deleted. (a) The *nif* clusters in *R.* sp. IRBG74. The deleted regions generated by the suicide plasmids pMR45–46 are marked (Methods). **(b)** Transfer of native *nif* constructs into *R.* sp. IRBG74. Nitrogenase activity was detected only from the transfer of the *R. sphaeroides nif* cluster into *R.* sp. IRBG74 MR17 (Δ*hsdR, recA*) but not into *R.* sp. IRBG74 MR19 (Δ*hsdR, recA* Δ*nif*). Expression of *A. caulinodans nifV* on the plasmid pMR49 in *R.* sp. IRBG74 MR17 was induced by 0.5 mM IPTG. The co-transfer of the complete *A. caulinodans nif* cluster on the two plasmids pMR19 and pMR20 did not yield activity in *R.* sp. IRBG74 MR17. Error bars represent standard deviation from three independent experiments on different days. Asterisk indicate ethylene production below the detection limit. Rsp, *R. sphaeroides*; Aca, *A. caulinodans*. **(c)** Plasmid maps used in (**b**).

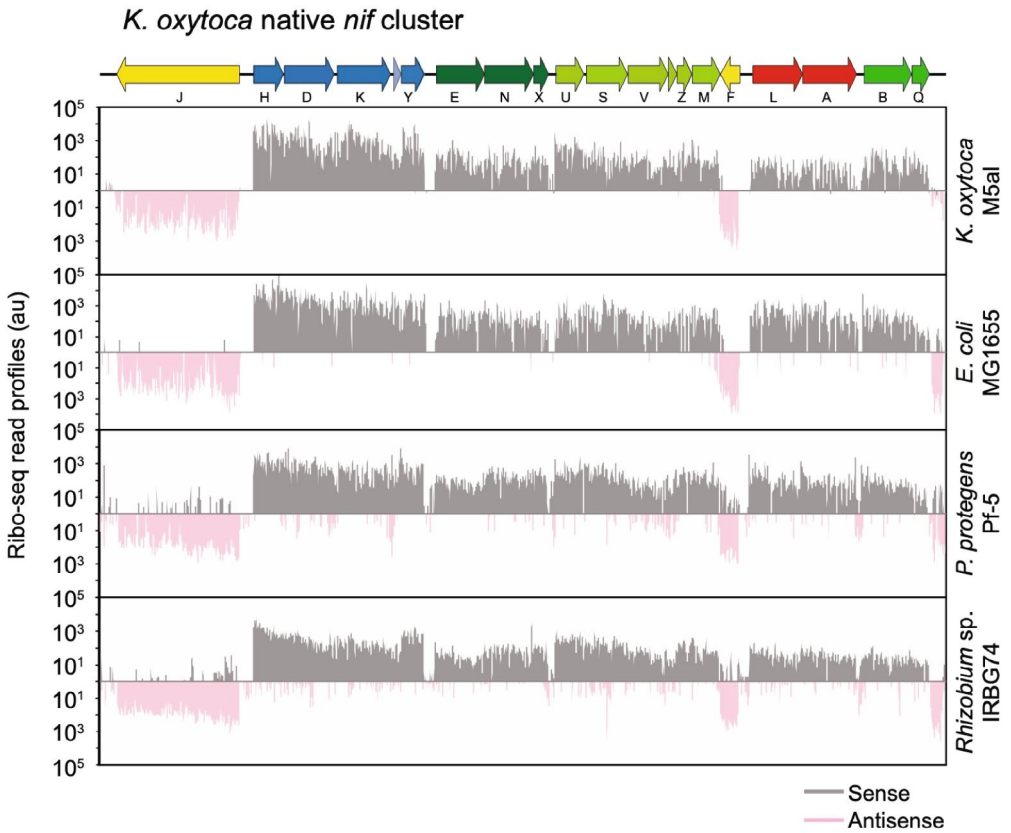

Extended Data Fig. 2 | Ribosome profiling data for the *K. oxytoca nif* cluster. Ribosome profiling data for the *K. oxytoca nif* cluster in its native host (top) and when transferred into different strains are shown.

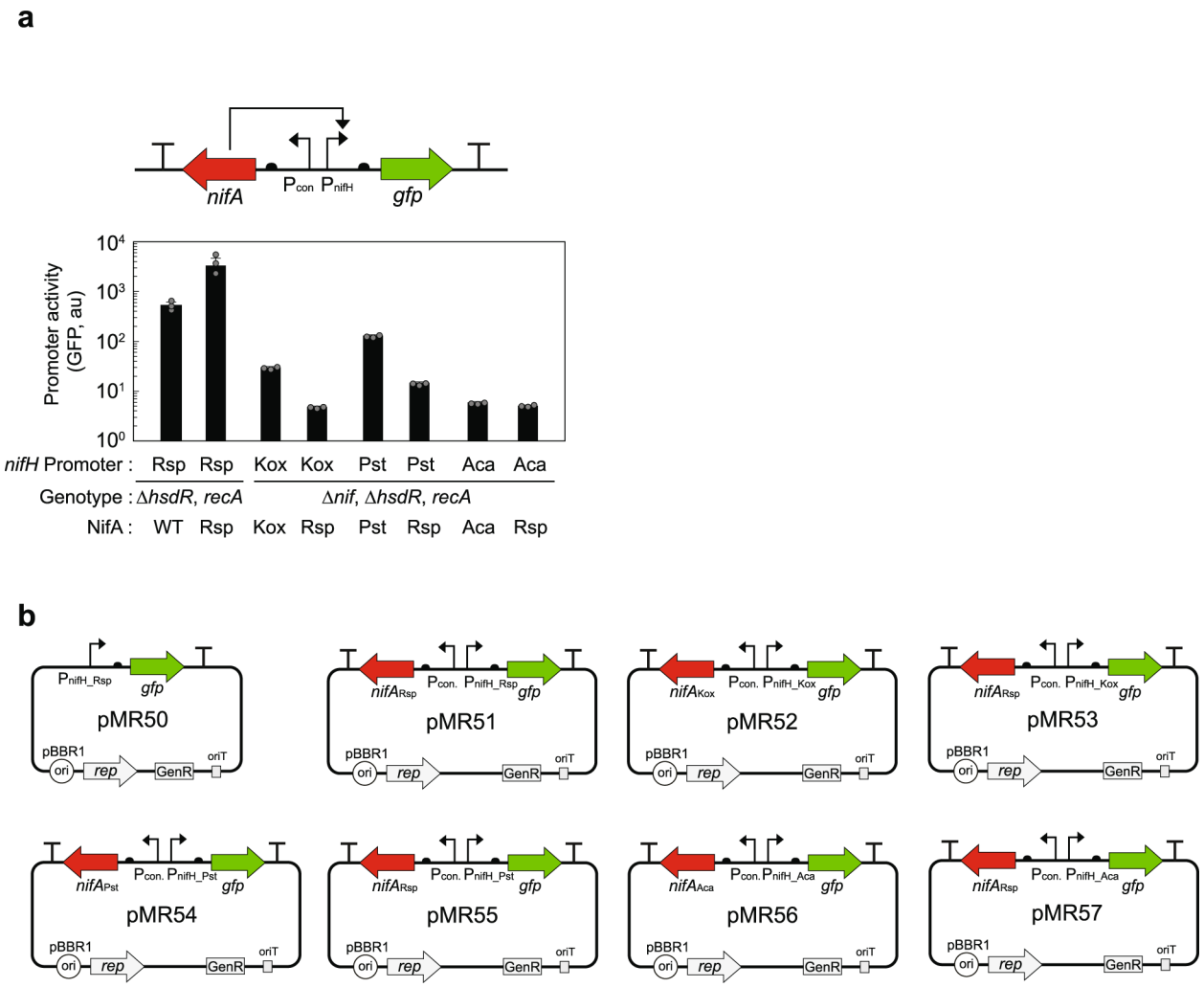

Extended Data Fig. 3 | The effect of NifA overexpression on the *nifH* promoter activity in *R.* sp. IRBG74. (a) The design of the reporter constructs used to measure *nifH* promoter activity shown. The *nifH* promoter activity was analysed in *R.* sp. IRBG74 using flow cytometry. Overexpression of *R.* sp. IRBG74 NifA increased the activity of the *R.* sp. IRBG74 *nifH* promoter but failed to complement or enhance the activities of the other *nifH* promoters including *K. oxytoca*, *P. stutzeri* and *A. caulinodans*. Error bars represent standard deviation from three independent experiments on different days. WT, wild-type; Rsp, *R.* sp. IRBG74; Kox, *K. oxytoca* M5al; Pst, *P. stutzeri* A1501; Aca, *A. caulinodans* ORS571 **(b)** Plasmid maps used to assess the effect of *nifA* overexpression in *R.* sp. IRBG74.

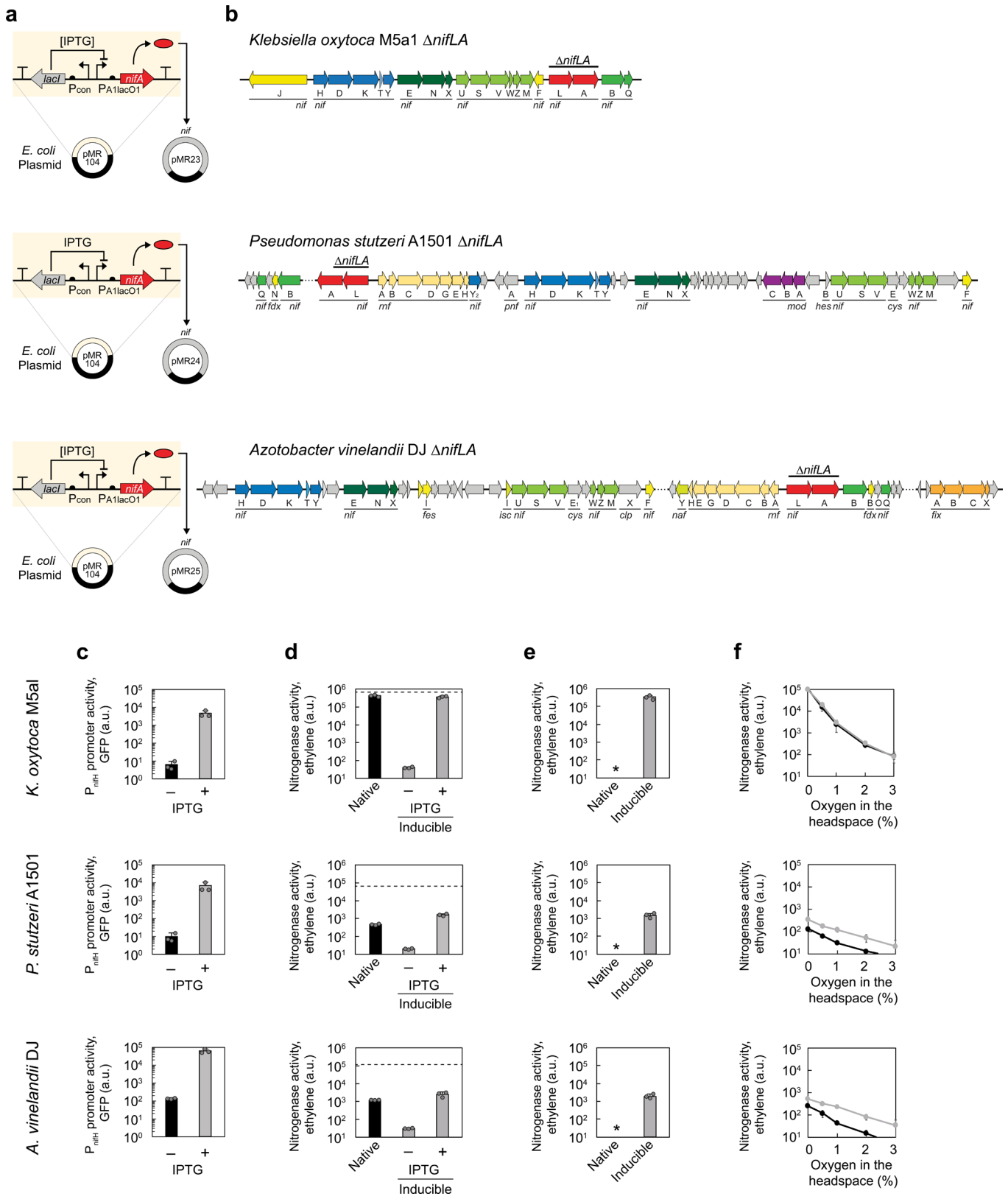

Extended Data Fig. 4 | See next page for caption.

Extended Data Fig. 4 | Nitrogenase activity when different inducible *nif* clusters are transferred to *E. coli* MG1655. (a) The same universal controller system based on *K. oxytoca nifA* was optimized and used for all three clusters (Supplementary Figure 15, 17b). The controller plasmid pMR104 and genetic parts are provided in Supplementary Table 3 and 4. **(b)** The *nif* clusters from *K. oxytoca*, *P. stutzeri*, and *A. vinelandii* are shown. The deleted regions corresponding the NifLA regulators are marked, and their corresponding genomic locations are provided in Supplementary Table 3. The dotted lines indicate that multiple regions from the genome were cloned and combined to form the *nif* cluster. The clusters were carried on the plasmids pMR23–25 (Supplementary Table 3). **(c)** The induction of the *nifH* promoters from each species by the controller are shown (+, 50 μM IPTG). **(d)** The nitrogenase activities of the native cluster (intact *nifLA*) are compared to the inducible clusters in the presence and absence of 50 μM IPTG. The dashed lines indicate the activity of the native clusters in the wild-type context (top to bottom, *K. oxytoca* M5al, *P. stutzeri* A1501 and *A. vinelandii* DJ). **(e)** Regulation of nitrogenase activity by ammonium. Ammonium tolerance of nitrogenase from the native (black bar) and inducible (grey bar) systems was tested in the presence of 17.1 mM ammonium acetate and 50 μM IPTG (inducible). Asterisks indicate ethylene production below the detection limit. **(f)** Regulation of nitrogenase activity by oxygen. The native *nif* cluster is compared to the inducible version including the controller plasmid and 50 μM IPTG. Nitrogenase activities were measured after 3 h of incubation at constant oxygen concentrations (0 to 3%) in the headspace (Methods). Error bars represent standard deviation from three independent experiments on different days.

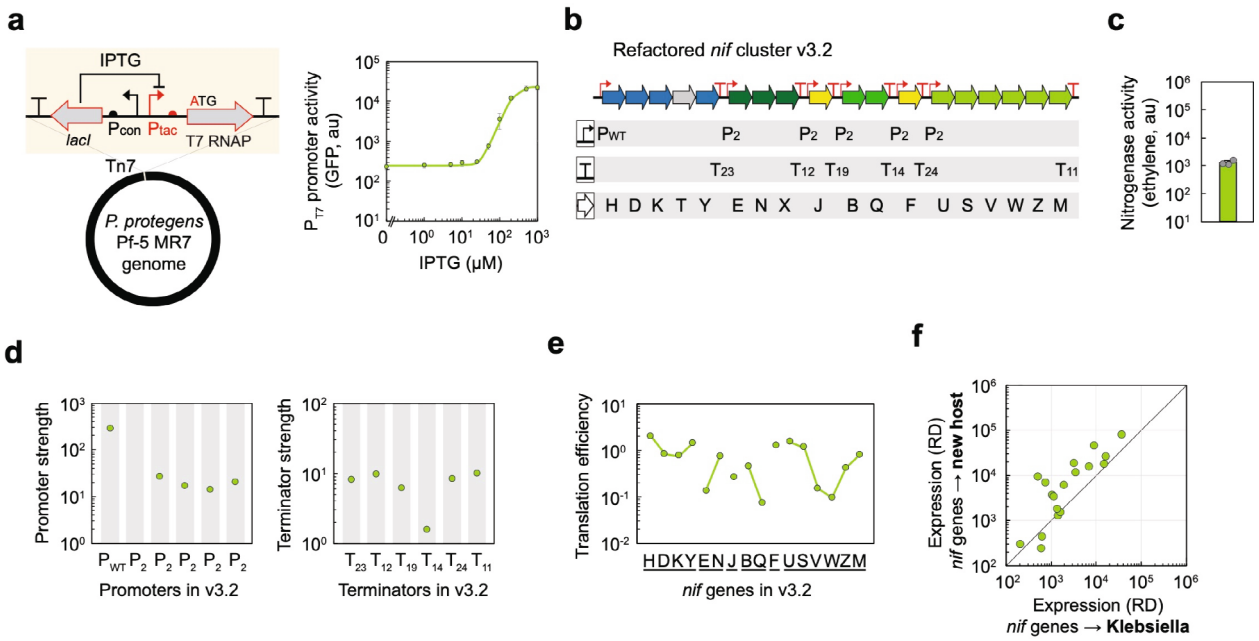

Extended Data Fig. 5 | Transfer of the refactored *nif* cluster v3.2 in *P. protegens* Pf-5. (**a**) Controllers whose output is T7 RNAP integrated on the genome of *P. protegens* Pf-5 are described. Substituted genetic parts for the controller optimization compared to the controller module pKT249 in *E. coli* MG1655 are highlighted in red. The response functions for the controllers with the reporter plasmid pMR81 was measured in the *P. protegens* Pf- 5 controller strain MR7. The controller driving the expression of GFP by the T7 promoter led to 96-fold induction by IPTG. (**b**) The genetic parts used to build the refactored v3.2 *nif* gene cluster are shown (provided in Supplementary Table 4). (**c**) The activity of the refactored *nif* cluster v3.2. Nitrogenase expression was induced by 1 mM IPTG. (**d**) The function of the transcriptional parts of the cluster v3.2 was analysed by RNA- seq (Supplementary Figure 18). The performance of the promoters (left) and terminators (right) was calculated (Methods). (**e**) The translation efficiency of the *nif* genes v3.2 as calculated using ribosome profiling and RNA-seq. Lines connect points that occur in the same operon. (**f**) The ribosome density (RD) is compared for the refactored v3.2 *nif* genes in *P. protegens* Pf-5 versus that measured for the *nif* genes from the native *K. oxytoca* cluster in *K. oxytoca* (→*Klebsiella*: $R^2 = 0.68$). Error bars represent standard deviation from three independent experiments on different days.

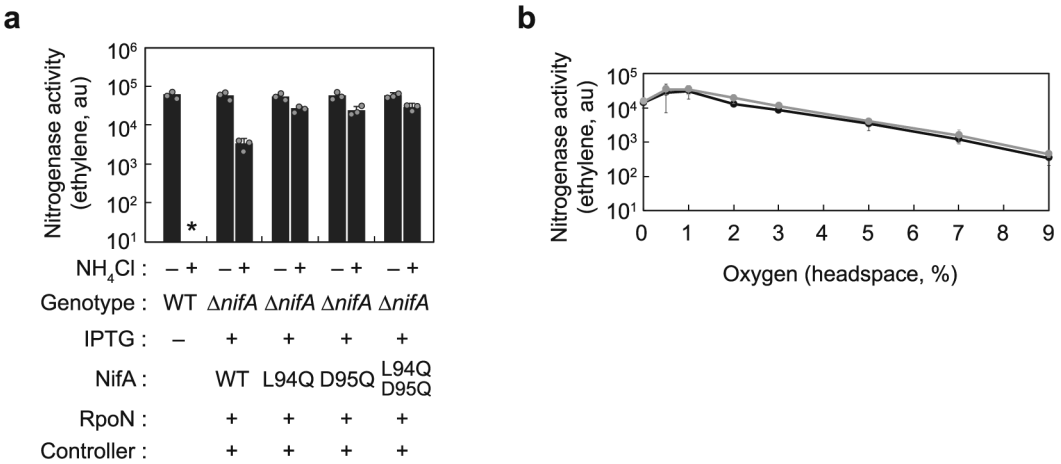

Extended Data Fig. 6 | Control of nitrogenase fixation in *A. caulinodans* ORS571 under changing environmental conditions. (a) The effect of the absence or presence of 10 mM ammonium chloride is shown. The WT NifA from *A. caulinodans* ORS571 is compared to different combinations of amino acid substitutions. NifA/RpoN expression is induced by 1 mM IPTG (+) for *A. caulinodans* Δ*nifA* containing the controller plasmid pMR124–127 (+). An asterisk indicates ethylene production below the detection limit. **(b)** The nitrogenase activity is shown as a function of the oxygen concentration in the headspace (Methods). The native *nif* cluster (wild-type *A. caulinodans* ORS571, black) is compared to the inducible version (grey) including the controller plasmid and 1 mM IPTG. Error bars represent standard deviation from three independent experiments on different days.

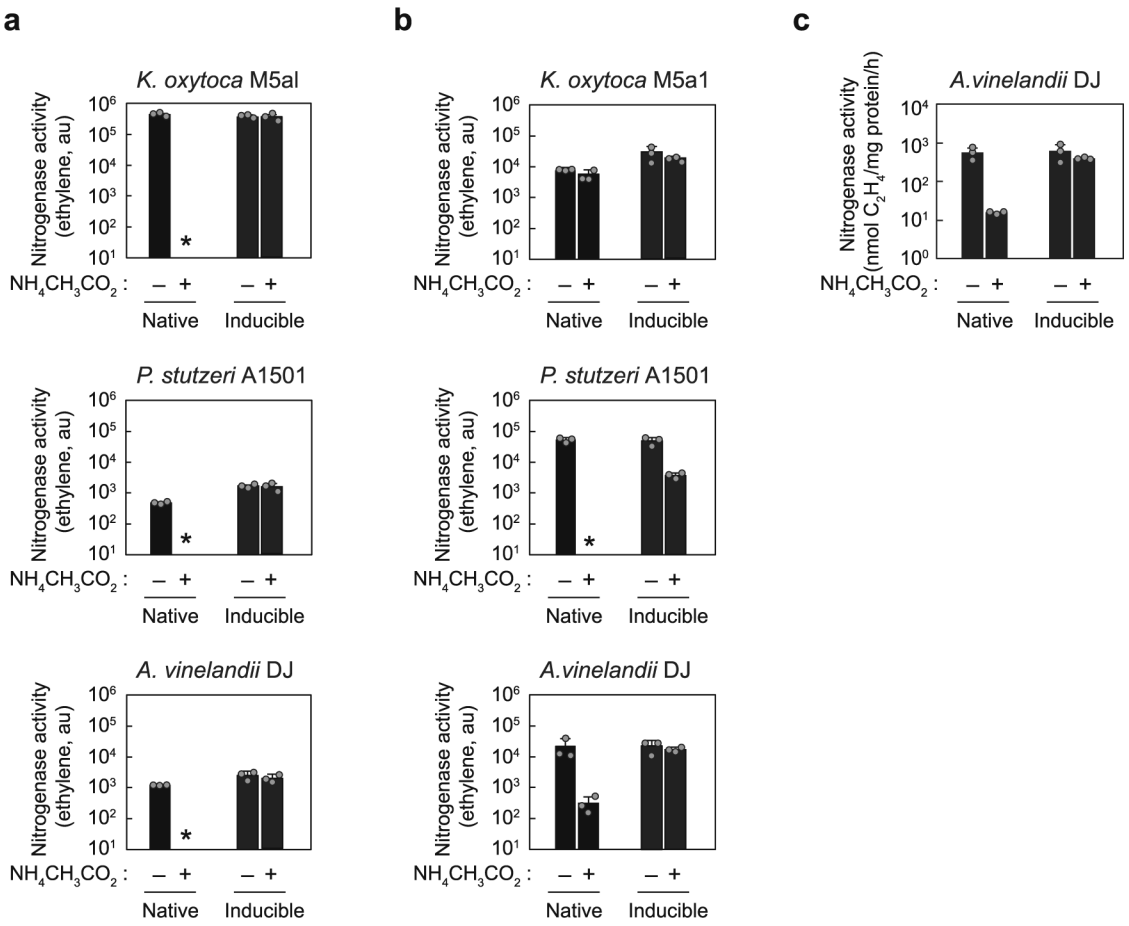

Extended Data Fig. 7 | Ammonium repression of the transferred *nif* clusters in *E. coli* MG1655 and *P. protegens* Pf-5. Nitrogenase sensitivity to ammonium was measured by acetylene reduction assay in the absence (-) or presence (+) of 17.1 mM ammonium acetate. The sensitivity of the native and inducible *nif* clusters in *E. coli* MG1655 **(a)** and *P. protegens* Pf- 5 **(b)**. Note that the data are from Fig. 4 and Supplementary Figure 8. **(c)** The specific nitrogenase activities of the native *A. vinelandii nif* cluster are compared to the inducible *A. vinelandii* cluster in the presence (+) and absence (-) of 17.1 mM ammonium acetate in *P. protegens* Pf-5. The *nif* clusters from the inducible version were induced by 50 μM and 0.5 mM IPTG in *E. coli* MG1655 and *P. protegens* Pf-5, respectively. Asterisks indicate ethylene production below the detection limit. Error bars represent standard deviation from three independent experiments on different days.

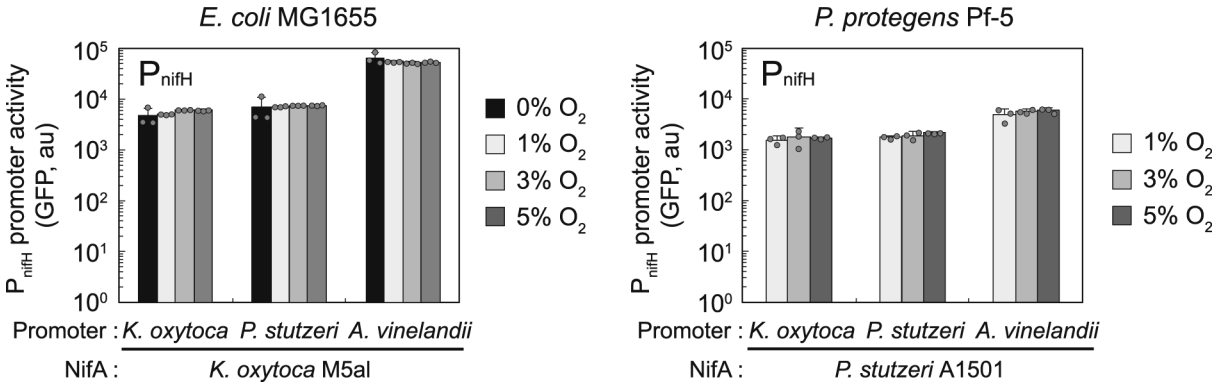

Extended Data Fig. 8 | The effect of oxygen on the activity of the *nifH* promoters. Expression from the *nifH* promoters was analysed in *E. coli* MG1655 containing the controller plasmid pMR104, *P. protegens* Pf-5 MR10 (for *K. oxytoca*) and MR9 (for *P. stutzeri* and *A. vinelandii*) at varying initial oxygen levels in the headspace. The three *nifH* promoters were induced with 0.05 mM IPTG and 0.5 mM IPTG in *E. coli* MG1655 and *P. protegens* Pf-5, respectively, and incubated at varying initial oxygen concentrations. Error bars represent standard deviation from three independent experiments on different days.

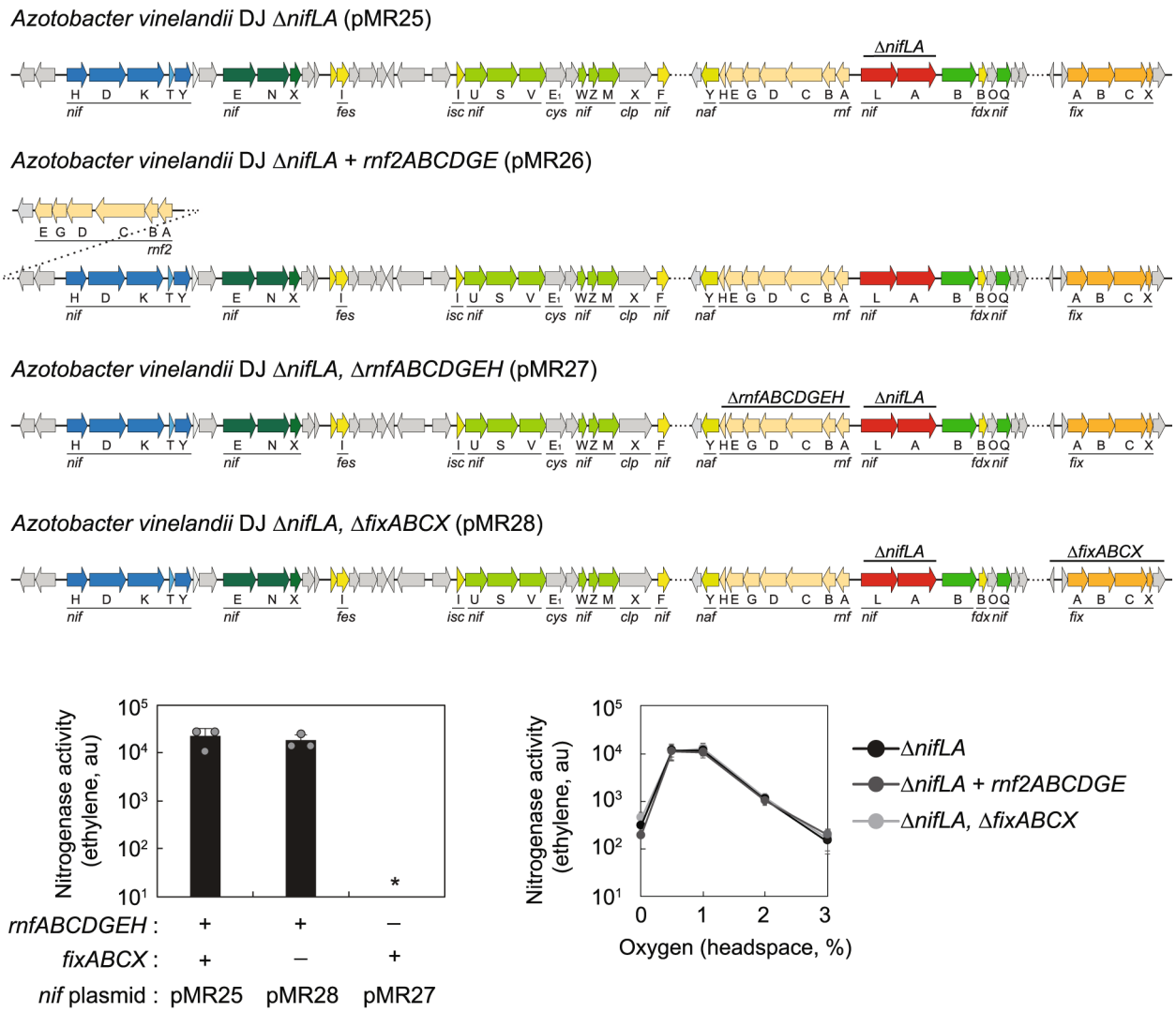

Extended Data Fig. 9 | The effect of the *rnf* and *fix* complex on nitrogenase activity. The modified *nif* clusters of *A. vinelandii* on the plasmids pMR25–28 were analysed in the controller strain *P. protegens* Pf-5 MR9. The deleted regions from the clusters were provided in Supplementary Table 3. Nitrogenase was induced with 0.5 mM IPTG. Dots in the DNA line indicate where multiple regions were cloned from genomic DNA and combined to form one large plasmid-borne *nif* cluster. An asterisk indicates ethylene production below the detection limit. Error bars represent standard deviation from three independent experiments on different days.

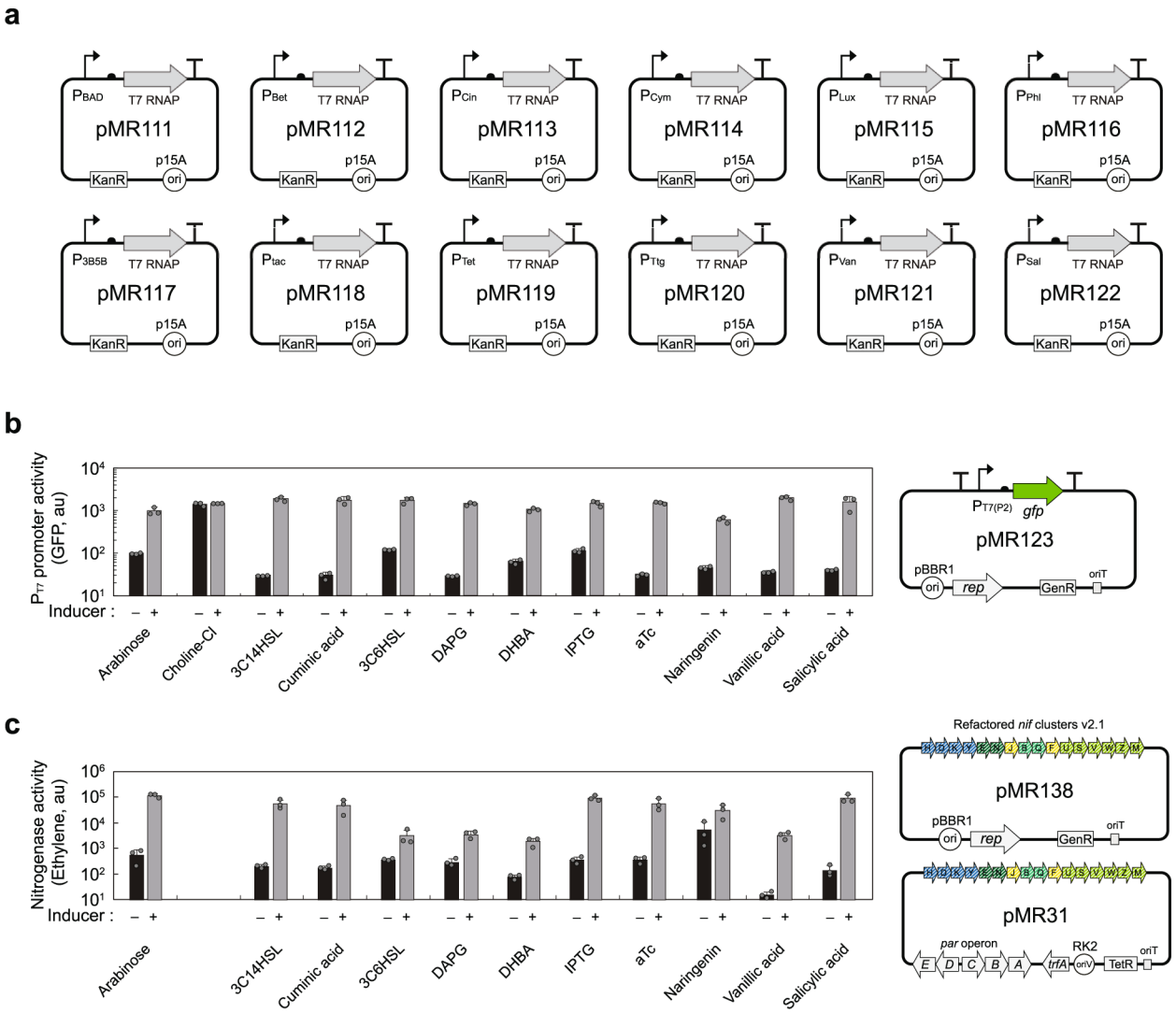

Extended Data Fig. 10 | Regulation of nitrogenase activity in the *E. coli* MG1655 'Marionette' strain. (a) Controller plasmids used to drive expression of T7 promoters. **(b)** Inducibility of the T7 promoter by the controller plasmids encoding T7 RNAP under the regulation of the 12 sensors was tested with a reporter plasmid pMR123 (right). **(c)** Inducible control of nitrogenase activity in response to 12 inducers was tested with each of 12 controller plasmid and the plasmid pMR138 (right) carrying the refactored *nif* cluster v2.1 on pBBR1 origin. The choline-Cl inducible system was omitted for activity assay as the system was not inducible. For the DAPG-, DHBA-, and vanillic acid-inducible system, the refactored cluster v2.1 was carried on a lower copy number plasmid pMR31 (right) as there was no colony formation from the transformation of the plasmid pMR138. The inducer concentrations are: 400 μM arabinose, 1 mM choline-Cl, 500 nM 3OC14HSL, 50 μM cuminic acid, 25 nM 3OC6HSL, 25 μM DAPG, 500 μM DHBA, 1 mM IPTG, 100 nM aTc, 250 μM naringenin, 50 μM vanillic acid, and 250 μM salicylic acid. Plasmid and genetic parts are provided in Supplementary Table 3 and 4. Error bars represent standard deviation from three independent experiments on different days.

nature research

Corresponding author(s): Christopher A. Voigt

Last updated by author(s): Mar 22, 2019

Reporting Summary

Nature Research wishes to improve the reproducibility of the work that we publish. This form provides structure for consistency and transparency in reporting. For further information on Nature Research policies, see Authors & Referees and the Editorial Policy Checklist.

Statistics

For all statistical analyses, confirm that the following items are present in the figure legend, table legend, main text, or Methods section.

n/a	Confirmed	
☐	☒	The exact sample size (*n*) for each experimental group/condition, given as a discrete number and unit of measurement
☐	☒	A statement on whether measurements were taken from distinct samples or whether the same sample was measured repeatedly
☐	☒	The statistical test(s) used AND whether they are one- or two-sided *Only common tests should be described solely by name; describe more complex techniques in the Methods section.*
☒	☐	A description of all covariates tested
☒	☐	A description of any assumptions or corrections, such as tests of normality and adjustment for multiple comparisons
☐	☒	A full description of the statistical parameters including central tendency (e.g. means) or other basic estimates (e.g. regression coefficient) AND variation (e.g. standard deviation) or associated estimates of uncertainty (e.g. confidence intervals)
☐	☒	For null hypothesis testing, the test statistic (e.g. *F*, *t*, *r*) with confidence intervals, effect sizes, degrees of freedom and *P* value noted *Give P values as exact values whenever suitable.*
☒	☐	For Bayesian analysis, information on the choice of priors and Markov chain Monte Carlo settings
☒	☐	For hierarchical and complex designs, identification of the appropriate level for tests and full reporting of outcomes
☒	☐	Estimates of effect sizes (e.g. Cohen's *d*, Pearson's *r*), indicating how they were calculated

Our web collection on statistics for biologists contains articles on many of the points above.

Software and code

Policy information about availability of computer code

Data collection	BD FACS DIVA software version 8.0.1 was used to collect all cytometry data.
Data analysis	FlowJo v10 (TreeStar Inc., Ashland, OR) was used to analyze cytometry data. Microsoft Excel version 16.30 was used to plot data. Geneious R9.0.5 was used to build phylogenetic trees. Scripts for analyzing '-omics' data are fully provided in Methods and freely available on request.

For manuscripts utilizing custom algorithms or software that are central to the research but not yet described in published literature, software must be made available to editors/reviewers. We strongly encourage code deposition in a community repository (e.g. GitHub). See the Nature Research guidelines for submitting code & software for further information.

Data

Policy information about availability of data

All manuscripts must include a data availability statement. This statement should provide the following information, where applicable:

- Accession codes, unique identifiers, or web links for publicly available datasets
- A list of figures that have associated raw data
- A description of any restrictions on data availability

Selected plasmids will be made available from Addgene. Strains and plasmids will be made available upon reasonable request from the corresponding author. RNA-seq and Ribo-seq data are available from Sequence Read Archive (accession code: PRJNA579767). The data that support the findings of this study will be available from the corresponding author upon reasonable request.

Field-specific reporting

Please select the one below that is the best fit for your research. If you are not sure, read the appropriate sections before making your selection.

☒ Life sciences ☐ Behavioural & social sciences ☐ Ecological, evolutionary & environmental sciences

For a reference copy of the document with all sections, see nature.com/documents/nr-reporting-summary-flat.pdf

Life sciences study design

All studies must disclose on these points even when the disclosure is negative.

Sample size	Statistical methods were not used to predetermine sample size.
Data exclusions	No data were excluded.
Replication	15N incorporation experiments (Figure 6e) and terminator characterization experiments (Supplementary Figure 5) were performed two times and all the other experiments were performed at least three times on different days. All attempts at replication were successful and presented in the data.
Randomization	Randomization is not relevant to this study. Data are quantitative and do not require subjective selection.
Blinding	Blinding is not relevant to this study. Data are quantitative and do not require judgment calls.

Reporting for specific materials, systems and methods

We require information from authors about some types of materials, experimental systems and methods used in many studies. Here, indicate whether each material, system or method listed is relevant to your study. If you are not sure if a list item applies to your research, read the appropriate section before selecting a response.

Materials & experimental systems

n/a	Involved in the study
☒	☐ Antibodies
☒	☐ Eukaryotic cell lines
☒	☐ Palaeontology
☒	☐ Animals and other organisms
☒	☐ Human research participants
☒	☐ Clinical data

Methods

n/a	Involved in the study
☒	☐ ChIP-seq
☐	☒ Flow cytometry
☒	☐ MRI-based neuroimaging

Flow Cytometry

Plots

Confirm that:

☐ The axis labels state the marker and fluorochrome used (e.g. CD4-FITC).

☐ The axis scales are clearly visible. Include numbers along axes only for bottom left plot of group (a 'group' is an analysis of identical markers).

☐ All plots are contour plots with outliers or pseudocolor plots.

☐ A numerical value for number of cells or percentage (with statistics) is provided.

Methodology

Sample preparation	Bacterial cells were diluted in phosphate buffered saline solution before measurement.
Instrument	BD LSR Fortessa
Software	BD FACS DIVA software v8 was used for data collection. FlowJo v10 (TreeStar Inc., Ashland, OR) was used for data analysis.
Cell population abundance	Gated populations consisted of at least 20,000 cells.

Gating strategy | Cells were gated: >100 side scatter height and >100 forward scatter height to capture all cells and remove background events.

☐ Tick this box to confirm that a figure exemplifying the gating strategy is provided in the Supplementary Information.